



8

BACTERIAL BIOMINERALIZATION

Kurt Konhauser¹ and Robert Riding²

¹Department of Earth & Atmospheric Sciences, University of Alberta, Edmonton, AB, T6G 2E3, Canada

²Department of Earth & Planetary Sciences, University of Tennessee, Knoxville, TN 37996, USA

8.1 Introduction

A number of living organisms form mineral phases through a process termed biominerization. Two end member mechanisms exist depending on the level of biological involvement. The first involves mineral formation without any apparent regulatory control. Termed 'biologically induced biominerization' by Lowenstam (1981), biominerals form as incidental by-products of interactions between the organisms and their immediate environment. The minerals that form through this passive process have crystal habits and chemical compositions similar to those produced by precipitation under inorganic conditions. By contrast, 'biologically controlled biominerization', the subject of Chapter 10, is much more closely regulated, and organisms precipitate minerals that serve physiological and structural roles. This process can include the development of intracellular or epicellular organic matrices into which specific ions are actively introduced and their concentrations regulated such that appropriate mineral saturation states are achieved. Accordingly, minerals can be formed within the organism even when conditions in the bulk solution are thermodynamically unfavourable. In this chapter we focus on the role of bacteria. Specifically, we examine the formation of iron oxyhydroxides and calcium carbonates throughout geological time, and explore how our understanding of modern biominerization processes is shedding new insights into the evolution of the Earth's hydrosphere–atmosphere–biosphere over long time scales.

8.2 Mineral nucleation and growth

The thermodynamic principles underpinning biological mineral formation, irrespective of whether it is induced or controlled, are the same as those involved in inorganic mineral formation. In all cases, before any solid can precipitate, a certain amount of energy has to be invested to form a new interface between the prospective mineral nucleus and both the aqueous solution and the underlying substrate upon which it is formed. The amount of energy required to do this can be viewed as an activation energy barrier. The standard free energy (G^0) of a solid is lower than that of its ionic constituents in solution, and if the activation energy barrier can be overcome, the reaction proceeds towards mineral precipitation. On the other hand, if the activation energy barrier is prohibitively high, metastable solutions persist until either the barrier is reduced or the concentration of ions are diminished.

Mineral nucleation involves the spontaneous growth of a number of nuclei that are large enough to resist rapid dissolution. Formation of these 'critical nuclei' requires a certain degree supersaturation wherein the concentration of ions in solution exceeds the solubility product of the mineral phase (see Stumm and Morgan, 1996, for details). Nucleation is termed homogeneous when critical nuclei form simply by random collisions of ions or atoms in a supersaturated solution. Such 'pure' solutions, however, rarely exist; in nature, most solutions contain a wide variety of competing solid and dissolved phases. In this regard, heterogeneous nucleation occurs when critical nuclei form on those solid phases.

After critical nuclei are formed, continued addition of ions is accompanied by a decrease in free energy, resulting in mineral growth. This process goes on spontaneously until the system reaches equilibrium.

Mineral growth typically favours the initial formation of amorphous solid phases that are characterized by their high degree of hydration and solubility, and lack of intrinsic form (Nielson and Söhnle, 1971). Accordingly, minerals such as amorphous silica ($\text{SiO}_2 \cdot n\text{H}_2\text{O}$), hydrated carbonate ($\text{CaCO}_3 \cdot \text{H}_2\text{O}$), or ferric hydroxide [Fe(OH)_3] will nucleate readily if the solution composition exceeds their solubility. In contrast, their respective crystalline equivalents, quartz (SiO_2), calcite (CaCO_3), and hematite (Fe_2O_3), have higher interfacial free energies. Therefore, they nucleate slowly at ambient temperatures, even in the presence of substrates favouring heterogeneous nucleation. Often the transition between amorphous and crystalline phases involves the precipitation of metastable phases.

The nucleation rate also affects the size of the critical nuclei formed. At high ion activities, above the critical supersaturation value, new surface area is created mainly by the nucleation of many small grains characterized by high surface area to mass ratios, a regime referred to as nucleation-controlled. At lower activities, surface area generation is crystal-growth controlled, with surface area increasing by the accretion of additional ions or atoms to existing grains. In a nucleation-controlled regime, the generation of new surfaces by nucleation occurs rapidly and causes the solution supersaturation to drop below the critical value needed for nucleation. This means that in nature, supersaturation above the critical value does not typically occur for lengthy periods of time. For silica precipitation as an example, if a concentrated silica solution were emitted from a hot spring vent, it would thermodynamically be supersaturated with regard to all silica phases, but because amorphous silica has the lower interfacial free energy it nucleates first despite quartz being the more stable phase with lower solubility. Then as amorphous silica nucleates it drives the dissolved silica concentration down to its critical value below which quartz nuclei formation is prohibitively slow.

Crystalline minerals that would otherwise be difficult or impossible to nucleate directly at low temperatures can circumvent activation energy barriers by making use of the more soluble precursors as templates for their own growth. Once they begin to grow, the crystals increase in surface area, and in doing so, they drive the proximal free ion concentration below the solubility of the amorphous precursor, causing it to dissolve (Steefel and Van Cappellen, 1990). However, despite thermodynamics predicting the transformation sequence based on energetics, they say nothing about the kinetics. Sometimes the reactions are relatively quick, such as the

formation of magnetite on ferric hydroxide. At other times, the reaction rates are immeasurably slow and the amorphous or metastable phases persist in sediments despite supersaturation with respect to more thermodynamically stable minerals. Those phases can show little discernible alteration for tens of millions of years until pressure-temperature changes associated with burial cause the reaction sequence to advance to the next stage (Morse and Casey, 1988). For example, amorphous silica skeletons (such as diatoms) deposited onto the seafloor slowly dissolve at shallow depths and re-precipitate as cristobalite, which remains stable to depths of hundreds of meters until it too transforms into quartz.

8.3 How bacteria facilitate biomimetic mineralization

Bacteria contribute significantly to the development of extremely fine-grained (often $<1\text{ }\mu\text{m}$ in diameter) mineral precipitates. All major mineral groups, whether metal oxyhydroxides, silicates, carbonates, phosphates, sulfates, sulfides, and even native metals, have been shown to precipitate as a consequence of bacterial activity. Although not directly associated with biologically controlled biomimetic mineralization, bacteria may influence the initial stages of mineralization in two significant ways:

8.3.1 Development of an ionized cell surface

Bacterial surfaces are highly variable, but commonly they have a cell wall that is overlain by additional organic layers, such as extracellular polymeric substances (EPS), sheaths and S-layers, which differ in terms of their hydration, composition and structure. In all cases, bacterial surfaces act as highly reactive interfaces. Organic ligands within the bacterial surface (such as carboxyl, hydroxyl, phosphoryl, sulfur and amine functional groups) deprotonate with increasing pH and thus impart the cells with a net negative surface charge (see Konhauser, 2007 for details). In its most simplistic form, deprotonation can be expressed by the following equilibrium reaction:



where B denotes a bacterium to which a protonated ligand type, A, is attached. The distribution of protonated and deprotonated sites can be quantified with the corresponding mass action equation:

$$K_a = \frac{[\text{B}-\text{A}^{-1}][\text{H}^{+1}]}{[\text{B}-\text{AH}]} \quad (8.2)$$

where K_a is the dissociation constant; $[\text{B}-\text{A}^{-1}]$ and $[\text{B}-\text{AH}]$ represent the respective concentrations of exposed deprotonated and protonated ligands on the bacterium (in mol l^{-1}); and $[\text{H}^{+1}]$ represents the activity of protons

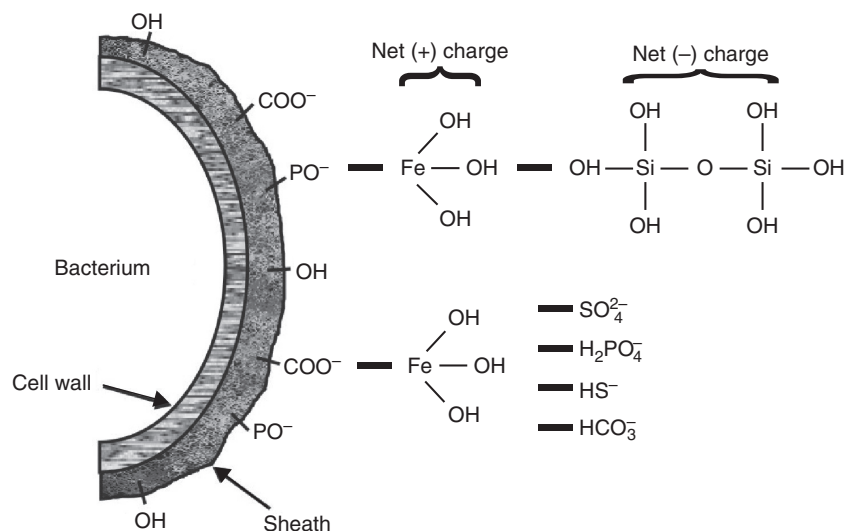


Figure 8.1 Schematic diagram of bacterial surface showing how the deprotonation of exposed functional groups leads to metal cation adsorption. Once bound, those cations can then react inorganically with dissolved anions in the external environment, such as silica, sulfate, phosphate, sulfide and bicarbonate. Depending on the anion available, different minerals may form on the bacterial surface.

in solution. Each functional group has its own K_a' and based on equation [8.2], the pH at which $[\text{B}-\text{A}^{-1}]$ and $[\text{B}-\text{AH}]$ are equivalent is known as the pK_a value, where $pK_a = -\log_{10} K_a$. At pH < pK_a the functional groups are predominantly protonated, and at pH > pK_a , they are predominantly deprotonated.

Due to these protonation–deprotonation reactions, the bacterial surface develops a negative surface charge at pH values characteristic of most natural environments, and in doing so, will become reactive towards charged cations and a number of mineral surfaces (Fig. 8.1). Some cations preferentially bind to different sites on the cell surface, and crucially, they are not equally exchangeable. For instance, trivalent (e.g. La³⁺, Fe³⁺) and divalent (e.g. Ca²⁺, Mg²⁺) metal cations are strongly bound to the cell wall of various bacteria, while monovalent cations (e.g. Na⁺, K⁺) are easily lost in competition with those metals for binding sites (Beveridge and Murray, 1976). This aspect is important to keep in mind – in natural systems, a multitude of cations and anions compete with one another for surface adsorption sites. Some of the most important factors that influence ion binding to cells are: (i) the composition of the solution, including pH and the activity of all ions; (ii) ligand spacing and their stereochemistry; (iii) ligand composition; and (iv) the balance between the initial electrostatic attractions between a soluble ion and the organic ligands, and the subsequent covalent forces that arise from electron sharing across a ion-ligand molecular orbital (see Williams, 1981).

One consequence of metal sorption is that the bound cation subsequently lowers the interfacial energy for heterogeneous nucleation of solid phases while

simultaneously decreasing the surface area of the nucleus that is in contact with the bulk solution. In this manner the bacterium catalyses mineral formation simply because it has bound cations on its outer surface. Those cations react with more ions, potentially leading to biominerization. With that said, bacteria only serve to enhance the precipitation kinetics in supersaturated solutions; they neither increase the extent of precipitation nor facilitate precipitation in undersaturated solutions (e.g. Fowle and Fein, 2001). The size of the mineral precipitate depends on a number of variables, including the concentration of ions and the amount of time through which the reactions proceed. The end result could be a bacterial wall that contains copious amounts of mineral precipitate, often approaching, or exceeding, the mass of the microorganism itself (Beveridge, 1984).

8.3.2 Metabolic processing

Each bacterium has a biogeochemical lifestyle that is optimally suited to its particular environmental conditions. And, all have two common objectives: to obtain energy and carbon. Energy can be captured from sunlight (phototrophy) or through the transfer of electrons from a reductant to an electron acceptor (chemotrophy). Carbon can be fixed through the reduction of CO₂ (autotrophy) or the consumption of pre-existing organic materials (heterotrophy). In all cases, the metabolic processes employed directly influence the chemistry and distribution of a wide range of elements. From a biominerization standpoint this is important because metabolism affects the redox and saturation states of the fluids around the living

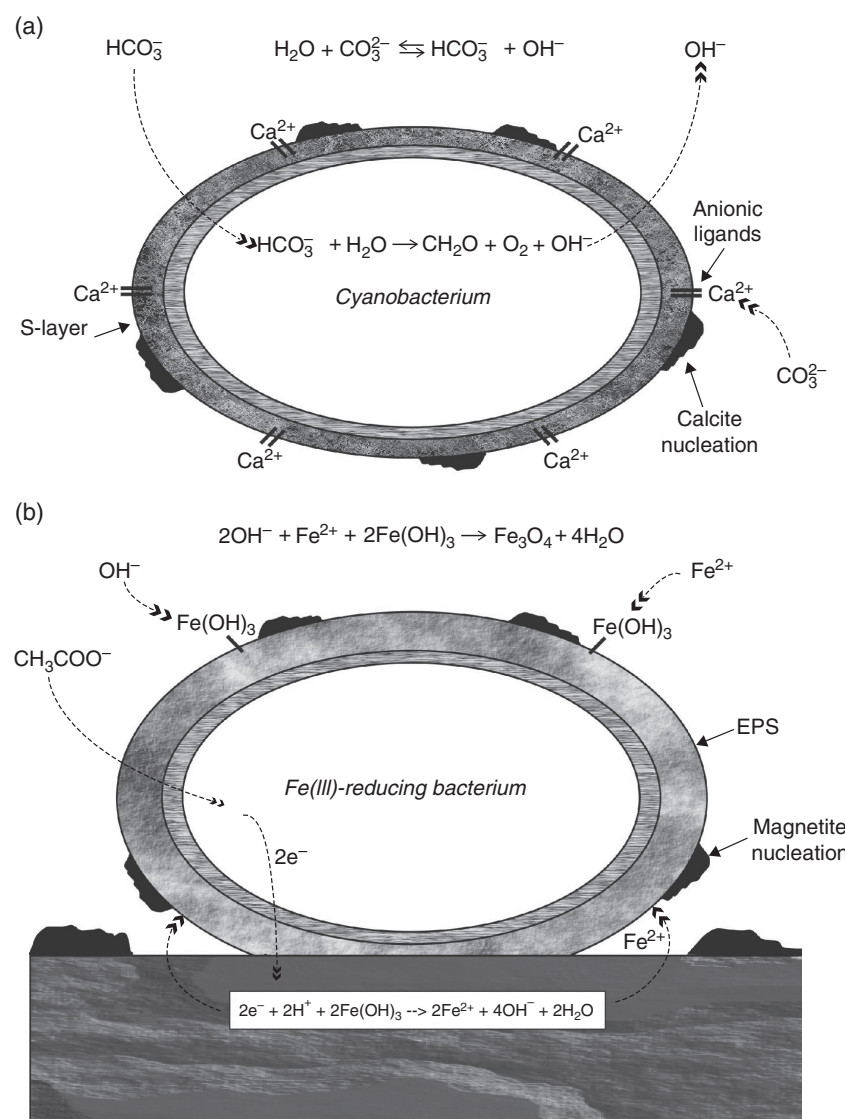


Figure 8.2 Schematic of metabolically-induced biomineralization in (a) cyanobacteria and (b) Fe(III)-reducing heterotrophs. In the cyanobacteria, uptake of the bicarbonate anion leads to excretion of OH^- , which in turn changes the alkalinity and inorganic carbon speciation proximal to the cell surface. The generation of carbonate anions and the pre-adsorption of calcium cations to the cell's sheath can then

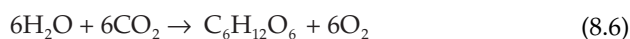
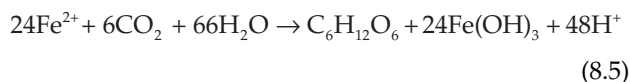
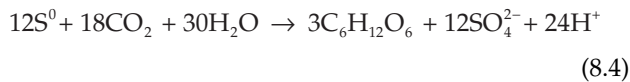
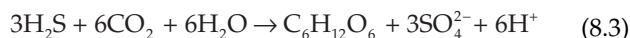
induce calcification. In the Fe(III)-reducing bacterium, release of $\text{Fe}(\text{II})$ from the ferric hydroxide substratum can promote magnetite formation both on the pre-existing mineral surfaces, but also on the cell surface if deprotonated ligands had adsorbed ferric iron. In both examples, the secondary minerals form as by-products of microbial metabolism – the cell itself did not control the mineralization process.

cells (Fig. 8.2). In this regard, the microenvironment surrounding each bacterium can be quite different from the bulk aqueous environment, and as a result, mineral phases form that would not normally be predicted from the geochemistry of the bulk fluid. It is important at this stage to point out that although these mineral phases are passively formed, there exists a grey zone between what constitutes minerals intimately associated with microbial biomass and the broader association of minerals formed by microbial activities changing local fluid chemistry.

8.3.2.1 Photoautotrophs

Phototrophic organisms use pigments to absorb sunlight and generate chemical energy. Two different processes of photosynthesis are: (1) anoxygenic photosynthesis, used by green bacteria, purple bacteria and heliobacteria; and (2) oxygenic photosynthesis, used by cyanobacteria, algae and plants. Anoxygenic species utilize hydrogen gas (H_2), hydrogen sulfide [reaction 8.3], elemental sulfur [reaction 8.4] and dissolved ferrous iron [reaction 8.5]. In oxygenic photosynthesis, the electrons

for CO_2 reduction come from splitting water into O_2 and electrons [reaction 8.6].



In reactions 8.3 and 8.4, the production of sulfate can affect the saturation state of sulfate minerals, and in some experimental studies, photoautotrophic bacteria can become encrusted by gypsum (CaSO_4), barite (BaSO_4) or celestite (SrSO_4) depending on the cations available to them in culture (e.g. Schultze-Lam and Beveridge, 1994). In reaction 8.5, and as discussed below in more detail, the oxidation of Fe(II) leads to the formation of dissolved Fe(III), which spontaneously hydrolyses at circumneutral pH values to form ferric hydroxide. This solid iron phase generally forms outside of cells where it can create difficulties for the bacterium because it acts as a physical barrier that inhibits diffusion of nutrients into the cell and of waste materials out of the cell. In fact, growth experiments with *Rhodomicobium vannielli* demonstrated that the ferric hydroxide crusts formed on the cell surface impeded further Fe(II) oxidation after two to three generations (Heising and Schink, 1998). Research is currently being conducted on various species of Fe(II)-oxidizing photoautotrophs to try to understand how they survive the effects of their own metabolism (e.g. Kappler and Newman, 2004; Hegler *et al.*, 2008).

Of all the reactions above, the one which arguably has had the greatest effect on life's evolution and diversification has been the generation of O_2 via oxygenic photosynthesis [reaction 8.6]. The ability of cyanobacteria to strip electrons from the virtually unlimited supply of water meant that they were not limited by reductants, and as a consequence, they were able to rapidly colonize the Earth's surface wherever sunlight was sufficiently present. As discussed in Chapter 7 (the Global Oxygen Cycle), the oxygen they produced gradually transformed the atmosphere and surface ocean from an anoxic to oxic state. This fuelled an oxygenated biosphere that profoundly altered the direction of evolution. This also significantly affected biominerization (see Chapter 18 on mineral evolution) because the oceans eventually attained sufficient concentrations of dissolved O_2 to oxidize reduced metals in the water column and top layers of sediment. For bacteria that had reduced metals

adsorbed to their outer surfaces, this meant that they now had to contend with the potential for metal oxidation and hydrolysis, leading to encrustation.

In addition, all phototrophs consume CO_2 , or more precisely, HCO_3^- – the predominant form of dissolved inorganic carbon in neutral to mildly alkaline waters (reaction 8.7). Excretion of the unconsumed products of this reaction, hydroxyl ions, into the external environment creates localized alkalinization around the cell surfaces (see Section 8.5.1.1). This in turn induces a change in the carbonate speciation towards the carbonate (CO_3^{2-}) anion (reaction 8.8), which ultimately may lead to the precipitation of calcium carbonate (Thompson and Ferris, 1990).

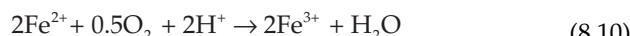


Cyanobacteria also provide reactive ligands to metal cations. Once bound, the cations can react with the dissolved carbonate to form mineral phases, such as aragonite or calcite (see Calcium Carbonates, below):



8.3.2.2 Chemolithoautotrophs

Similar to the photoautotrophs, chemolithoautotrophs use CO_2 as their source of carbon, however, sunlight is not their source of energy. Instead, they oxidize reduced inorganic substrates coupled to a terminal electron acceptor, usually O_2 . For biominerization, the most important reactions include the oxidation of Fe(II) (reaction 8.10), Mn(II) (reaction 8.11) and CH_4 (reaction 8.12).



Ferrous iron oxidation is discussed in detail below. The development of manganese oxides occurs in the same types of present-day oxic-anoxic interfacial environments where ferric hydroxide forms, but because Mn(II) is not subject to such rapid oxidation as Fe(II), at circumneutral pH most Mn(II) oxidation results from microbial catalysis (Ehrlich, 2002). At marine hydrothermal sites, MnO_2 forms as crusts around seafloor vents and where hot fluids percolate up through the sediment (Mandernack and Tebo, 1993). Analyses of the hydrothermal plumes emanating from the southern Juan de

Fuca Ridge have also shown that the particulate fraction is largely composed of bacterial cells encrusted in iron and manganese, with Fe-rich particles near the vent and Mn-rich particles further off-axis (Cowen *et al.*, 1986).

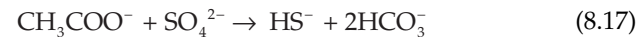
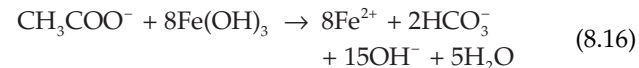
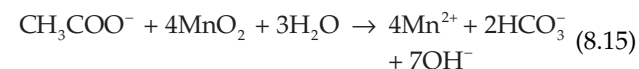
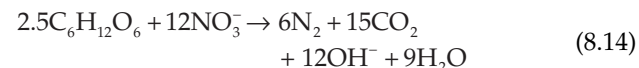
One type of bacteria, the methanotrophs, makes a living from oxidizing methane to CO_2 . They are widespread in marine sediment where methane from underlying anoxic zones diffuses upwards into the overlying oxic zone, allowing them to use O_2 to oxidize methane. There is, however, another group of methanotrophs that lives in anoxic sediments and, in conjunction with other bacteria, facilitates the oxidation of methane via concomitant reduction of sulfate (reaction 8.12). This reaction is significant in limiting the release of methane to the atmosphere, and in some marine sediment it can account for nearly 100% of the downward SO_4^{2-} flux (D'Hondt *et al.*, 2002). The oxidation of methane (and other hydrocarbon gases) under anoxic conditions leads to an increase in alkalinity and the subsequent precipitation of aragonite and Mg-calcites as cements that line cavities in the sediment, and as carbonate nodules that tend to show repeated zonation with framboidal pyrite (FeS_2). The precipitation of carbonates can even produce seafloor topographic features with up to several meters of relief (Michaelis *et al.*, 2002). These precipitates serve as a major inorganic carbon sink, and help stabilize the microbial community by cementing the soft sediment and forming a hard, solid substratum that can be used for attachment by symbiotic macrofauna, such as tubeworm, clam and mussel colonies. Methane oxidation coupled to sulfate reduction further generates HS^- that not only provides an inorganic energy source for sulfur-oxidizing bacteria, such as *Beggiatoa*, *Thiothrix* and *Thioploca*, but it also reacts with $\text{Fe}(\text{II})$ to precipitate as iron monosulfide (reaction 8.13), and it is not uncommon to observe pyritized remains of bacteria (Sassen *et al.*, 2004).



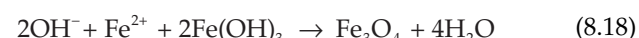
8.3.2.3 Chemoheterotrophs

There are several chemoheterotrophic reactions that play a profound role in sediment diagenesis, including reduction of dissolved (O_2 , NO_3^- , SO_4^{2-} , CO_2) and solid (MnO_2 and ferric oxyhydroxides) substrates. Of those, the reduction of nitrate (reaction 8.14), manganese(IV) (reaction 8.15), ferric iron (reaction 8.16) and sulfate (reaction 8.17) have substantial biomineralization potential because they increase pore water alkalinity, raising the saturation state for calcium carbonate minerals (Canfield and Raiswell 1991a). The net effect is precipitation of early diagenetic carbonate minerals that are relatively stable once formed, and not subject to rapid

recycling by redox reactions in the same way as sulfides and oxides (Irwin *et al.*, 1977).



The reduction of ferric iron minerals also produces an increase in the concentration of Fe^{2+} in suboxic sediment pore waters, with a peak at the boundary between the Fe(III) and sulfate reduction zones. Some of this ferrous iron may diffuse upwards to be re-oxidized to ferric hydroxide inorganically by either NO_3^- or MnO_2 (e.g. Myers and Nealson, 1988). However, in marine sediment most ferrous iron is removed from solution by reaction with hydrogen sulfide produced by the underlying populations of sulfate reducing bacteria (reaction 8.17). This forms metastable iron monosulfide minerals, such as mackinawite, that are precursors to pyrite (Berner, 1984). When abundant ferric iron is available (enough to keep HS^- concentrations down) other ferrous iron-containing minerals can precipitate. One such mineral is magnetite (Fe_3O_4) that can occur as tiny (10–50 nm), rounded, poorly crystalline particles on cell surfaces. Although the actual role that Fe(III)-reducing bacteria play in magnetite formation remains unresolved, the adsorption of Fe^{2+} (produced during ferric iron reduction) to the remaining ferric hydroxide appears to be the key step in the precipitation process (reaction 8.18) (Lovley, 1990).



Other minerals that form in cultures of Fe(III)-reducing bacteria are siderite (FeCO_3) and vivianite ($\text{Fe}_3[\text{PO}_4]_2$). Marine siderite has been linked to the activity of Fe(III)-reducing bacteria, since they generate both ferrous iron and bicarbonate. By contrast, when sulfate reduction rates exceed Fe(III) reduction rates, enough HS^- is produced to precipitate iron monosulfide minerals instead (FeS has lower solubility than FeCO_3). Therefore, the precise spatial distribution of Fe(III) reduction and sulfate reduction in marine sediments controls whether siderite and/or pyrite form (e.g. Coleman, 1985). The formation of vivianite in many ways resembles that of siderite in that Fe^{2+} concentrations must exceed those of HS^- . It also requires that soluble phosphate is made available through oxidation of

organic matter, the dissolution of phosphorous-bearing solid phases or through reduction of phosphorous-adsorbing Fe(III) oxides (Krom and Berner, 1980).

8.3.3 Microbial interactions in nature

A wide variety of microbial 'biominerals' exist in sedimentary environments (see Konhauser, 2007, chapter 4). Those formed passively are entirely dependent upon the chemical composition of the fluids in which they are growing; a mineral phase will form only if the requisite solutes are immediately available. Conversely the same bacterium in a different environment could form a different mineral phase altogether. For example, it is well known that the anionic ligands comprising a cell's surface can form covalent bonds with dissolved ferric iron species, which in turn can lead to charge reversal at the cell surface. Invariably, this positive charge will attract anionic counter-ions from solution (recall Fig. 8.1). So, in the sediment, iron adsorption to a bacterium may lead to the precipitation of an iron sulfate precipitate in the oxic zone, whereas another bacterium may instead form an iron sulfide at depth, when conditions become reducing.

It is also important to stress that in any given environment different bacteria co-exist, often utilizing different metabolic pathways. Consequently, one species may contribute to the formation of a mineral phase, while others in close proximity may have a completely different impact. Using iron as an example, bacteria in the oxic zone may oxidize dissolved Fe(II) leading to ferric hydroxide precipitation, while bacteria growing in suboxic layers may be involved in the reduction of that ferric mineral, facilitating Fe(II) release, and potentially the formation of mixed ferrous-ferric minerals, such as magnetite, or completely reduced ferrous mineral phases, such as siderite, pyrite or vivianite.

The impact that biominerization has on elemental cycling in aqueous and sedimentary environments cannot be overstated. Present-day C, Ca, Fe, Mg, Mn, P, S and Si cycles are all strongly affected by biominerizing processes. Although individual biomineral grains are micrometres in scale, if one adds the total amount of biominerizing biomass, it is not difficult to imagine how they can be significant in partitioning metals from the hydrosphere into the sedimentary system. The precipitation of iron oxides and carbonate minerals by bacteria are especially relevant throughout Earth's history. For example, the extensive record of banded iron formation (BIF), from 3.8 to 0.5 billion years ago, testifies to the enormous magnitude of ferric iron deposition to the seafloor. Given that they are chemical precipitates, BIF have been used as proxies for paleo-oceanic conditions (e.g. Bjerrum and Canfield, 2002; Konhauser *et al.*, 2009; Planavsky *et al.*, 2010). On a similar, or even larger,

scale calcium carbonate minerals represent the final products in the weathering of silicate minerals, and a long-term sink for atmospheric carbon dioxide. In the following sections, we explore the importance of bacterial biominerization of both iron oxyhydroxides and calcium carbonates.

8.4 Iron oxyhydroxides

The most widespread iron biominerals is ferric hydroxide (also loosely referred to as ferrihydrite). It forms in any environment where Fe(II)-bearing waters come into contact with O₂. This includes mine wastes, springs and seeps, freshwater and marine sediment, soils and subsurface fractured rock, hydrothermal vents, and water distribution systems, to name just a few (see Konhauser, 1998). Fossils that resemble modern iron depositing bacteria have been found in laminated black cherts and hematite-bearing jaspillites from several Early Proterozoic banded iron formations (Robbins *et al.*, 1987). There is also circumstantial evidence suggesting that microbial activity was directly involved in the initial deposition of iron sediment, which later consolidated to make BIF (e.g. Konhauser *et al.*, 2002; Kappler *et al.*, 2005; Posth *et al.*, 2008).

The role bacteria play in ferric hydroxide formation can range from completely passive to that actively facilitated. Yet, by current definitions, this process is not considered biologically controlled because the bacterium does not manage all aspects of the mineralization process. In the most passive of examples, ferrous iron transported into an oxygenated environment at circumneutral pH spontaneously reacts with dissolved oxygen to precipitate inorganically as ferric hydroxide on available nucleation sites. Bacteria provide such sites by their mere presence, and over a short period of time the submerged communities can become completely encrusted in amorphous iron hydroxide as abiological surface catalysis accelerates the rate of mineral precipitation. Initial microscopic observations of such samples often indicate a paucity of bacteria, but staining the iron-rich sediment with fluorescent dyes for nucleic acids (e.g. acridine orange) often reveals high bacterial densities closely associated with the iron precipitates (e.g. Emerson and Revsbech, 1994a). In other cases, where bacteria are more actively involved, ferric hydroxide can form through the oxidation and hydrolysis of cell-bound ferrous iron (Fe²⁺) and dissolved ferric ion species [e.g. Fe³⁺, Fe(OH)²⁺; Fe(OH)₂⁺; Fe(OH)₃], or when local pH and redox conditions around cells are altered by their metabolic activity. In fact, the iron-coating on cells grown in Fe-rich cultures can be sufficiently dense to visualize the bacteria under the transmission electron microscope (TEM) without the standard use of metal stains (Fig. 8.3a).

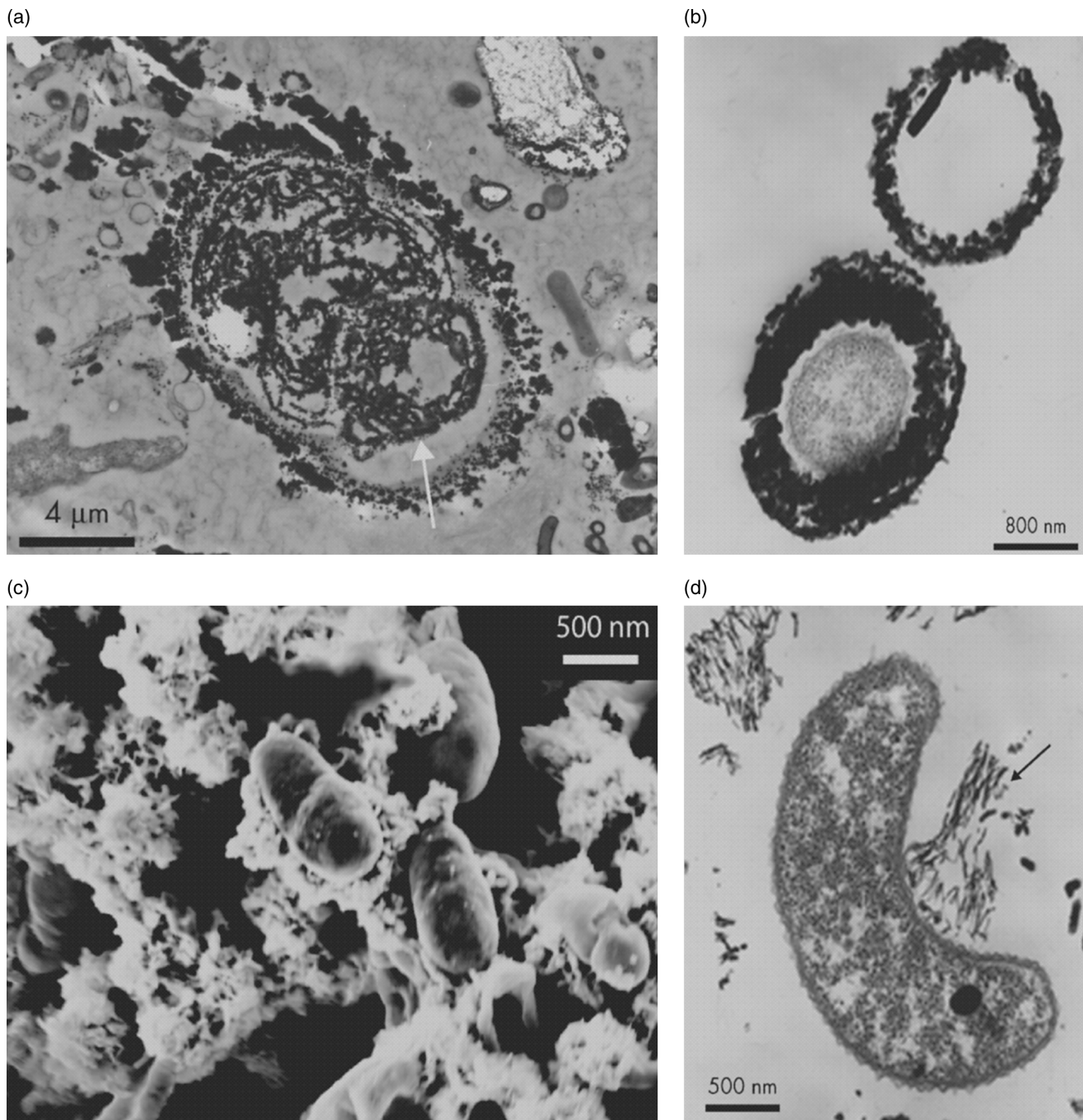


Figure 8.3 Transmission electron micrographs (TEM) and scanning electron micrographs (SEM) of iron hydroxide-cell assemblages. (a) a lysed bacterial cell with remnants of organic material retained within an iron hydroxide coating (from Konhauser, 2007). (b) two ferric hydroxide encrusted *Leptothrix ochracea* cells from an iron seep in Denmark. The cross section shows one ensheathed cell and one abandoned

sheath (from Emerson, 2000). (c) the phototrophic Fe(II)-oxidizing *Rhodobacter ferrooxidans* attached to ferric hydroxide particles it generated during anoxygenic photosynthesis using dissolved Fe(II) (from Konhauser *et al.*, 2005). (d) image of *Gallionella ferruginea*, showing a portion of its stalk (arrow) attached to the cell (from Emerson, 2000).

Because of the ubiquity of iron biomimetic mineralization in nature, it has been suggested that under circumneutral conditions any microorganism that produces anionic ligands will non-specifically adsorb cationic iron species or fine-grained iron hydroxides from the surrounding waters (Ghiorse, 1984; Glasauer *et al.*, 2001). This is not unexpected given that the zero point of charge of pure ferric hydroxide is 8–9. Ferric hydroxide also develops on the organic remains of dead cells, implying that iron biomimetic mineralization can occur independently of cell physiological state.

8.4.1 Chemoheterotrophic iron mineralization

A number of microorganisms, the so-called iron depositing bacteria, facilitate iron mineralization by having surface ligands that promote Fe(II) oxidation, although it is not believed that they gain energy from the process (see Emerson, 2000 for review). The most common visible inhabitant of many freshwater, low-oxygenated iron seeps is *Leptothrix ochracea*. This chemoheterotroph frequently forms thick filamentous layers comprising a mass of tubular sheaths encrusted in iron. In an iron seep in Denmark, cell counts of 10^8 – 10^9 cells cm^{-3} promote iron accumulation rates of 3 mm day^{-1} (Emerson and Revsbech, 1994b), an extremely rapid sedimentation rate compared to the deposition of clastic sediments in marginal marine environments.

An interesting observation is that it is rare to find intact filaments of *L. ochracea* cells inside their sheaths (e.g. Fig. 8.3b). This correlates well with experiments showing that *Leptothrix* continuously abandons its sheath at a rate of 1 – $2\text{ }\mu\text{m min}^{-1}$, leaving behind sheaths 1–10 cells in length that continue to deposit ferric hydroxide. This would seem to indicate that the bacteria use sheath secretion to avoid becoming permanently fixed in the mineral matrix (van Veen *et al.*, 1978). Other heterotrophic bacteria, such as filamentous species of *Sphaerotilus*, *Crenothrix*, *Clonothrix* and *Metallogenium*, as well as unicellular cocci of the *Siderocapsaceae* family, can induce ferric hydroxide precipitation through oxidation of organic iron chelates. In this manner, they use the organic carbon of such ligands as an energy source, resulting in the liberation and hydrolysis of ferric iron (Ghiorse and Ehrlich, 1992).

8.4.2 Photoautotrophic iron mineralization (photoferrotrophy)

As discussed above, and in detail in chapter 6, some anoxygenic photosynthetic bacteria are capable of oxidizing Fe(II) to Fe(OH)_3 , using light for energy for CO_2 fixation (recall reaction 8.5). This process could be described as ‘facilitated biomimetic mineralization’ because ferric iron precipitates as a direct result of the metabolic

activity of the microorganisms (Fig. 8.3c). These bacteria are phylogenetically diverse and include green sulfur bacteria (e.g. *Chlorobium ferrooxidans*), purple non-sulfur bacteria (e.g. *Rhodobacter ferrooxidans*) and purple sulfur bacteria (e.g. *Thiodictyon* sp.). All strains are mesophilic, with maximum growth rates at $23\text{ }^\circ\text{C}$, but are able to survive temperatures as low as $4\text{ }^\circ\text{C}$, while their growth is optimal at pH values around 7 (Hegler *et al.*, 2008). All experimental strains are also able to oxidize Fe(II) at very low light levels (down to 50 lux), which means that they can grow in light regimes befitting the photic zone of ocean water to depths of 100 m, or greater (Kappler *et al.*, 2005).

Ferrous iron can be used as an electron donor by these bacteria because the standard electrode potential for $\text{Fe}^{2+}/\text{Fe}^{3+}$ (+0.77 V) is applicable only at very acidic pH, whereas at more neutral pH, the potential shifts to less positive values due to the low solubility of Fe^{3+} (Ehrenreich and Widdel, 1994). Photoferrotrophic growth can also be sustained by the presence of soluble ferrous iron minerals, such as siderite and iron monosulfide, but not insoluble minerals, such as vivianite, magnetite or pyrite (Kappler and Newman, 2004).

A current area of interest involves understanding how photoferrotrophs survive the mineralization process. Some have speculated that the cells prevent encrustation by creating a localized pH gradient outside the cell so that the Fe(III) remains soluble and can diffuse away from the cell until it reaches a less acidic environment (Kappler and Newman, 2004). Others have suggested that organic iron-chelating molecules may be involved in Fe(III) release by Fe(II)-oxidizing phototrophs (Straub *et al.*, 2001). The story has been complicated by the recent observation that Fe(II) is oxidized in the periplasm of some photoferrotrophs, which not only means that dissolved Fe(II) is brought into the cell, but that some dissolved form of Fe(III) must be excreted or else the periplasm would fill with ferric hydroxide (Jiao and Newman, 2007).

8.4.3 Chemolithoautotrophic iron mineralization

The formation of iron hydroxides may also stem from the ability of some chemolithoautotrophic bacteria to oxidize ferrous iron as an energy source (recall reaction 8.10). Although most enzymatic oxidation of Fe(II) occurs at extremely low pH, such as in acid mine drainage environments, the activity of *Acidithiobacillus ferrooxidans* or *Leptospirillum ferrooxidans* generally does not promote *in situ* ferric hydroxide precipitation because the Fe^{3+} formed remains soluble until more alkaline pH conditions ensue. However, at neutral pH, and under low oxygen concentrations, chemolithoautotrophic Fe(II) oxidation (e.g. by *Gallionella ferruginea*) does lead to high rates of iron

mineralization (e.g. Søgaard *et al.*, 2000). In fact, the extracellular stalk can become so heavily encrusted with amorphous ferric hydroxide that the majority of its dry weight is iron (Fig. 8.3d).

Similar to *L. ochracea*, *Gallionella* species are common inhabitants of iron springs, and where they are abundant, the stalk material appears to form the substratum upon which subsequent Fe(II) oxidation occurs. Nonetheless, actively growing *Gallionella* and *Leptothrix* populations appear to occupy separate microniches within the same iron seep environments; the former preferring areas of sediment with lower oxygen concentrations (Emerson and Revsbech, 1994a). In wells, water pipes and field drains of water distribution systems, the large amount of iron precipitated by *Gallionella* has long been recognized as a cause of serious clogging problems (e.g. Ivarson and Sojak, 1978).

In anoxic environments, Fe(II) oxidation has also been shown to proceed with nitrate as the electron acceptor (Straub *et al.*, 1996). What was intriguing about the Straub study was the observation that nitrate-reducing species, that had not previously been grown in iron media, exhibited the capacity for ferrous iron oxidation, implying that this form of microbial oxidation may be commonplace. Indeed, bacteria that reduce nitrate with ferrous iron have now been recovered from wetlands (Weber *et al.*, 2006); shallow marine hydrothermal systems (e.g. Haenbrandl *et al.*, 1996); and even deep sea sediments (e.g. Edwards *et al.*, 2003).

One particularly interesting feature about this form of metabolism is that most of the described nitrate-dependent Fe(II)-oxidizing strains depend on an organic co-substrate (e.g. acetate) and so far, only one truly lithoautotrophic nitrate-reducing strain has been isolated in pure culture. 16S rRNA gene analyses from the Straub study showed that this culture consists of four organisms, including three chemoheterotrophic nitrate-reducing bacteria (*Parvibaculum lavamentivorans*, *Rhodanobacter thiooxidans* and *Comamonas badia*), plus a fourth organism related to the chemolithoautotrophic Fe(II)-oxidizing bacterium *Sideroxydans lithotrophicus* (Blothe and Roden, 2009). The complexity of this culture potentially suggests that a consortium of organisms is needed for autotrophic Fe(II) oxidation coupled to nitrate-reduction.

8.4.4 Hydrothermal ferric hydroxide deposits

Perhaps the most striking example of ferric hydroxide biomineratization is at marine hydrothermal settings. Ferric iron minerals commonly precipitate directly on the seafloor, where subsurface mixing of hydrothermal fluids with infiltrating seawater produce metal-rich solutions that range in temperature from near ambient deep sea (~2 °C) to around 50 °C. The deposits themselves

range from centimetre-thick oxide coatings formed by diffuse venting through underlying basalts or solid-phases sulfides to more voluminous oxide mud deposits (Juniper and Tebo, 1995).

Extensive deposits of ferric hydroxide-rich muds have been described from a number of submarine hydrothermal sites, including: (1) the shallow waters around the island of Santorini, (2) the Red and Larson Seamounts on the East Pacific Rise, and (3) the Loihi Seamount of the Hawaiian archipelago. The Santorini site is likely the most unambiguous example of ferric hydroxide precipitation because the mineralized stalks of *Gallionella ferruginea* occur so abundantly in the bottom sediment (Holm, 1987). The Red Seamount is characterized by an abundance of bacterial filaments, some of which have morphologies reminiscent of Fe(II)-oxidizing bacteria, e.g. twisted ribbons like *Gallionella ferruginea*, twisted spirals like *Leptospirillum ferrooxidans* and straight sheaths similar to *Leptothrix ochracea*. Although there is no direct evidence supporting enzymatic Fe(II) oxidation, indications of a microbial role in mineralization comes from the fact that the hydrothermal waters in which these deposits form are not conducive to rapid ferrous iron oxidation (Alt, 1988). The Loihi Seamount is the newest shield volcano at Hawaii. The impact of high Fe(II)/low H₂S emissions is apparent from the extensive deposits of ferric hydroxide that encircle the vent orifices, where anoxic hydrothermal waters mix with oxygenated seawater, and in the peripheral regions where visible mats are present. Initial microscopic analyses revealed that both deposits were rich in Fe-encrusted sheaths, similar in appearance to those of *Leptothrix ochracea* (Karl *et al.*, 1988). Since then, a number of studies have shown that the iron deposits have abundant microbial populations associated with them, up to 10⁸ cells mg⁻¹ (wet weight) of mat material, and that many of the cells are novel microaerophilic Fe(II)-oxidizers (Emerson *et al.*, 2010). Two interesting findings that have recently come from studies at Loihi are: (1) that the majority of ferric iron deposited around the vents is directly or indirectly attributable to bacterial activity (Emerson and Moyer, 2002), and (2) the bulk of the energy utilized by the seafloor chemolithoautotrophic communities derives from the iron released via hydrothermal emissions, and not oxidative weathering of the underlying basalts (Templeton *et al.*, 2009).

8.4.5 Geobiological implications

8.4.5.1 Evidence for ancient Fe(III)-precipitating microbes

For much of Earth's history the oceans were iron-rich (see Chapter 6 on the Global Iron Cycle), with dissolved Fe(II) concentrations estimated around 0.02 mM

(Holland, 1973; Morris, 1993); some 1,000 to 10 000 times modern seawater values. The ferruginous nature of the Precambrian oceans is manifested by the presence of BIF, chemical sedimentary rocks that were precipitated throughout the Archean and Paleoproterozoic. They then disappeared for a billion years before reappearing in association with episodes of global glaciation during the Neoproterozoic (Bekker *et al.*, 2010). BIF are characteristically laminated, with alternating Fe-rich (hematite, magnetite, and siderite) and silicate/carbonate (chert, jasper, dolomite and ankerite) minerals. Banding can often be observed on a wide range of scales, from coarse macrobands (meters in thickness) to mesobands (centimetre-thick units) to millimetre and submillimetre layers. Some deposits, such as in the 2.5 Ga Dales Gorge Member, in the Hamersley Group of Western Australia, show laterally contiguous layers up to a hundred in extent, suggesting that BIF were deposited uniformly over areas of tens of thousands of square kilometers (Trendall, 2002). The layering in BIF has been attributed to seasonal or decadal episodic hydrothermal pulsation and/or upwelling of anoxic, Fe-rich waters into semi-restricted basins already saturated with dissolved silica (Morris, 1993; Posth *et al.*, 2008).

Despite the lack of direct evidence, it is becoming increasingly accepted that microorganisms were involved in the primary oxidation of Fe(II) to Fe(III) in BIF. Two possible roles for bacteria are envisioned. The first is based on the production of O₂ by cyanobacteria, or their predecessors, as first proposed by Cloud (1965). In this model, these microorganisms would have flourished when Fe(II) and nutrients were available and passively induced the precipitation of ferric hydroxide through their metabolic activity and/or by sorbing aqueous Fe species to the anionic ligands exposed on their cell surfaces (Konhauser, 2000). Under an anoxic atmosphere, this O₂ could have been confined to local 'oxygen oases' associated with cyanobacterial blooms in coastal settings (Cloud, 1973). Once oxygen was present, chemolithoautotrophic Fe(II) oxidizers (using O₂ as the oxidant) could also have contributed to biogenic Fe mineral precipitation. For instance, Holm (1989) speculated that oxidation of dissolved Fe(II) by ancient forms of *Gallionella ferruginea* would have been kinetically favoured in an ocean with limited free oxygen because inorganic rates of Fe(II) oxidation at circumneutral pH are sluggish under microaerobic conditions (e.g. Liang *et al.*, 1993).

The second hypothesis, first elaborated on by Hartman (1984), is that anoxygenic photosynthetic bacteria may have coupled the C and Fe cycles prior to the evolution of oxygenic photosynthesis. The ability of primitive anoxygenic bacteria to oxidize Fe(II) is supported by the isolation of various marine and freshwater purple and green phototrophic bacteria that can use Fe(II) as a

reductant for CO₂ fixation (recall discussion above). Models based on the Fe(II) oxidation rates of these strains under varying environmental conditions further demonstrate the plausibility of photoferrotrophy as a means for primary BIF precipitation (Konhauser *et al.*, 2002; Kappler *et al.*, 2005). Indeed, the ferric iron minerals that these strains produce are comparable with the Fe(III) precipitates that probably were deposited as primary BIF minerals. In particular, photoferrotrophs produce poorly crystalline ferric hydroxide, which carries a net positive charge (Kappler and Newman, 2004). Such biogenic minerals are expected to bind to organic carbon (e.g. cells), leading to deposition of cell-mineral aggregates on the seafloor. Metabolically-driven synsedimentary reactions and subsequent burial diagenesis would then transform the aggregates. Ferric hydroxide would either dehydrate to hematite or be reduced to magnetite and/or siderite, while organic carbon would be oxidized to CO₂. These reactions have been used to account for the lack of organic carbon in BIF deposits and the isotopic composition of the secondary minerals in BIF (Walker, 1984; Konhauser *et al.*, 2005).

One issue that any biological model for BIF must consider is when did cyanobacteria and photoferrotrophs evolve? Although the timing of cyanobacterial evolution is widely debated, the general consensus leans towards 2.8 to 2.7 Ga based on several lines of evidence from the rock record. For instance, based on geochemical constraints, it has been proposed that stromatolites from the 2.7 Gyr old Tumbiana Formation in Western Australia were formed by phototrophic bacteria that used oxygenic photosynthesis (Buick, 1992). This view is bolstered by the earliest recognized microfossil assemblage of colonies of filamentous and coccoid cells, from the 2.6 Gyr Campbell Group, South Africa, that are similar in appearance to modern oscillatoriacean cyanobacterial genera, such as *Phormidium* or *Lyngbya* (Altermann and Schopf, 1995). Bitumens from the 2.6 Gyr Marra Mamba Iron Formation of the Hamersley Group in Western Australia have yielded abundant amounts of 2α-methylhopanes, derivatives of prominent lipids in cyanobacteria (methyl-bacteriohopanepolyols), which imply cyanobacteria existed in the oceans at that time (Brocks *et al.*, 1999; Summons *et al.*, 1999), while extremely ¹²C-rich kerogens from marine sediments aged 2.7–2.6 Ga have been attributed to the metabolic coupling of methane generation and its subsequent oxidation with O₂ by a group of aerobically respiring bacteria called methanotrophs (Hayes, 1983; Eigenbrode and Freeman, 2006). Most recently, trace metal speciation in 2.6 Ga black shales points towards oxygen availability in marine waters possibly several hundred meters deep (Kendall *et al.*, 2010).

In terms of anoxygenic photosynthetic bacteria, molecular phylogenetic analyses of a number of

enzymes involved in (bacterio)-chlorophyll biosynthesis suggest that anoxygenic photosynthetic lineages are almost certain to be more deeply rooted than oxygenic cyanobacterial ones (Xiong, 2006). Recent studies also indicate that anoxygenic phototrophs represent a considerable fraction of biomass in modern stromatolite communities, and the recently demonstrated construction of stromatolite-like structures by the anoxygenic phototroph *Rhodopseudomonas palustris*, challenges the notion that stromatolites only indicate cyanobacteria in the geologic record (e.g. Bosak *et al.*, 2007). Furthermore, unique biomarkers for anoxygenic phototrophs, remnants of specific light-harvesting pigments, have recently been found in Paleoproterozoic strata, offering intriguing evidence for their presence on ancient Earth (Brocks *et al.*, 2005). It is interesting to note that 2-methylbacteiohopanes have also been identified in significant quantities in modern anoxygenic phototrophic Fe(II)-oxidizers (Rashby *et al.*, 2007), making the case for Fe(II)-oxidizing phototrophs at 2.7 Ga just as plausible as that for O₂-producing cyanobacteria.

8.4.5.2 What BIF tell us about ancient seawater

In natural systems where trace element sequestration by ferric hydroxide particles results from a continuum of adsorption and co-precipitation reactions (Ferris *et al.*, 1999), lumped-process distribution coefficient models can be used to relate the concentration of an element in the ferric hydroxide precipitate to the dissolved concentration present at the time of precipitation (Dzombak and Morel, 1990). This predictive aspect of the sorption reactions has subsequently been exploited to better understand the BIF record with respect to ancient seawater composition, and ultimately, nutrient availability for the ancient marine biosphere. Two examples have recently been addressed in the literature.

The first used BIF compositional data and phosphate partitioning coefficients between modern seawater and hydrothermal iron hydroxide precipitates to hypothesize that primary productivity in the Archean oceans may have been limited during BIF deposition by the strong adsorption of phosphate to the iron particles precipitating in the photic zone (Bjerrum and Canfield, 2002). The starvation of cyanobacteria would have had a knock-on effect by limiting oxygen production, which in turn, helped delay the eventual oxygenation of the atmosphere. While this study was quite revolutionary in its linking of seawater geochemistry to the productivity of the biosphere via the BIF record, its interpretation was likely complicated by the fact that the Archean oceans were also highly siliceous. Dissolved silica has a higher propensity for sorbing onto ferric hydroxides than dissolved phosphate, which means that in an

amorphous silica-saturated ocean, phosphate levels may well have been sufficient to support plankton growth (Konhauser *et al.*, 2007). A recent compilation of P content in BIF and other iron-rich sediments through time has added an extra dimension to the phosphate story. Based on a five-fold increase in the phosphate concentrations in BIF from 750–630 Myr ago, a time coincident with two possible global ‘Snowball Earth’ glaciations, Planavsky *et al.* (2010) suggested that enhanced chemical weathering during deglaciation led to increased phosphate supply to the oceans, which in turn, led to greater cyanobacterial productivity, increased organic carbon burial, and eventually a transition to more oxidizing conditions in the oceans and atmosphere. This sequence of steps could then have facilitated the rise of animal life.

The second example used molar Ni/Fe ratios preserved in BIF over time to demonstrate the dynamic links between the physical evolution of the planet to changes in the biosphere and atmosphere. Konhauser *et al.* (2009) observed that the nickel content of BIF changed dramatically over time; from high Ni content between 3.8 and 2.7 billion years ago, dropping to about half that value between 2.7 and 2.5 billion years ago, and then slowly approaching modern values by 0.55 billion years ago. The large drop in Ni availability reflected a progressively cooling mantle and the eruption of less Ni-rich volcanic rocks (e.g. komatiites). Decreased komatiite production meant less Ni was dissolved into the oceans to become incorporated into BIF. The drop in seawater Ni at 2.7 Ga would have had profound consequences for microorganisms that depended on it, that being methane-producing bacteria, the methanogens. These bacteria have a unique Ni requirement for many of their essential enzymes, and a deficiency in the metal would have decreased their metabolism, resulting in less methane production. Crucially, methanogens have been implicated in controlling oxygen levels on the ancient Earth because the methane they produced was reactive with oxygen and kept oxygen levels low. So as long as methane was abundant, oxygen could not accumulate in the atmosphere, and indeed, it is believed that methane production must have dropped to enable the rise of atmospheric oxygen some 2.4 billion years ago, the so-called ‘Great Oxidation Event’ (Zahnle *et al.*, 2006).

8.5 Calcium carbonates

Bacterial carbonates are long-lived and locally abundant sediments that record both bacterial growth and the environmental factors that promote calcite/aragonite (CaCO₃) and dolomite [CaMg(CO₃)₂] precipitation in, on and around bacteria and the organic matter that they produce. These sediments include biogenic water

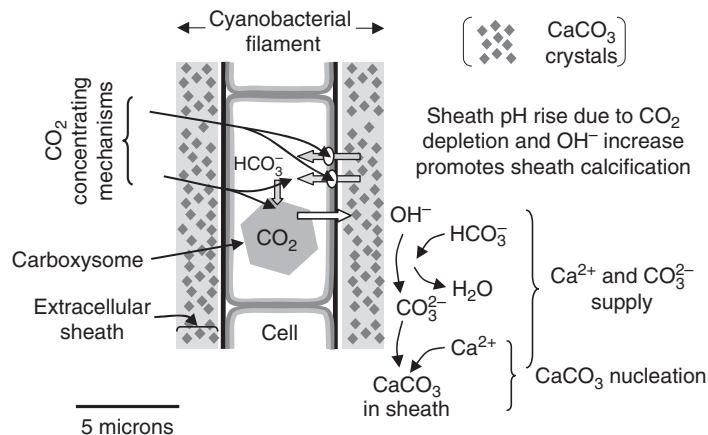


Figure 8.4 Schematic of *in vivo* cyanobacterial sheath calcification driven by CCM-enhanced photosynthesis (from Riding 2006, based on information from Miller and Colman, 1980; Thompson and Ferris, 1990; Merz, 1992; Price *et al.*, 1998; Kaplan and Reinhold, 1999; Badger and Price, 2003). Cyanobacterial CCMs include active uptake of HCO₃⁻ and its conversion to CO₂ for fixation by Rubisco in the carboxysome. This releases OH⁻, which elevates the pH of fluids within the sheath pH, and ultimately promotes calcification.

column precipitates (whittings) that produce carbonate mud deposits on lake and sea floors, and a variety of *in situ* benthic deposits, most notably stromatolites. Present-day bacterial carbonates are deposited in diverse environments, but their geological history is best recorded in marine sedimentary rocks and extends through at least the past 2.5 Gyr, and possibly 1 Gyr more.

Calcification (CaCO₃ precipitation) by bacteria is not obligatory and it shows close dependence on environmental conditions, particularly the carbonate saturation state of ambient waters. It is therefore a good example of 'induced', as opposed to 'controlled' biomimetication. This reliance can be used to interpret changes in past environmental conditions, including the concentrations of dissolved inorganic carbon (e.g. CO₂, HCO₃⁻) and sulfate that are required by key bacterial metabolic processes such as photosynthesis and sulfate reduction, respectively. Thus, secular patterns of bacterially induced calcification provide insights into long-term changes in Earth's surface environments that include seawater and atmospheric composition.

8.5.1 Cyanobacteria

Cyanobacterial calcification occurs when CaCO₃ crystals nucleate within the extracellular sheath or on the cell wall and EPS. These distinct styles of calcification have differing paleobiological and sedimentary consequences. Sheath impregnation by CaCO₃ crystals can create discrete microfossils such as *Girvanella* that are known since the mid-Proterozoic. By contrast, crystals formed at outer cell surfaces of bacteria that lack sheaths can subsequently be released into the water column as small loose particles or aggregates. These form milk-like, fine-grained suspensions (whittings) that settle out to accumulate as carbonate mud on lake and sea floors. However, they are not known to contain features that

reflect a specifically cyanobacterial origin and so they are difficult to discriminate from carbonate mud formed in other ways, such as by breakdown of algal and invertebrate skeletons.

8.5.1.1 Calcification mechanisms

Despite considerable progress, much remains to be understood concerning the factors influencing cyanobacterial calcification. Variation in calcification between strains within the same environment suggest intrinsic effects involving, for example, metabolic rates and mechanisms, growth stages, cell structure, type of EPS, and surface charge characteristics (Golubic, 1973). Nonetheless, three critically important factors have been recognized: (1) photosynthetic uptake of bicarbonate ions, (2) adsorption of Ca²⁺ to cell surfaces, and (3) ambient saturation state with respect to calcium carbonate.

As discussed in Section 8.3.2.1, photosynthetic uptake of bicarbonate results in pH increase near the cell (recall reaction 8.8) (Miller and Colman, 1980). Bicarbonate uptake is regarded as a response to low CO₂ availability and can be experimentally induced in cyanobacteria at atmospheric CO₂ levels below ~0.36% (Badger *et al.*, 2002). The bicarbonate is transformed into CO₂ within the cell and this process is termed a CO₂-concentrating mechanism (CCM). It involves a series of steps: active HCO₃⁻ transport into the cell, its intracellular conversion to CO₂, and the resulting external release of OH⁻ ions. OH⁻ release is the critical process driving calcification because it raises pH, potentially promoting CaCO₃ nucleation when ambient carbonate saturation is already elevated (reaction 8.19). Thus, pH increase near cyanobacterial cells resulting from CCM induction can stimulate both whiting production and sheath calcification (Riding, 2006) (Figs 8.4 and 8.5).



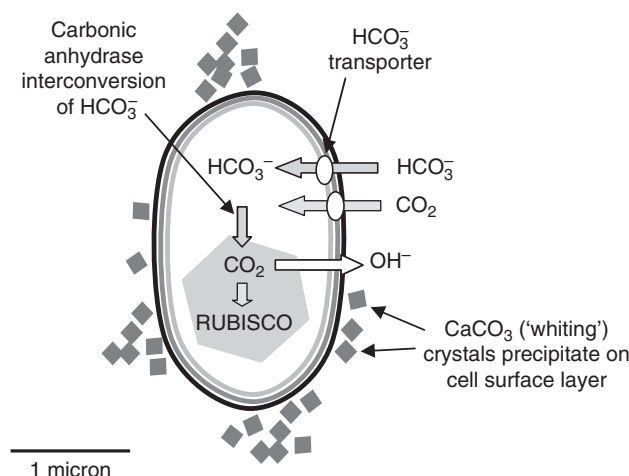


Figure 8.5 Where a sheath is lacking, CCMs promote CaCO_3 precipitation on the surface layer of individual picoplanktonic cyanobacterial cells (see Thompson and Ferris, 1990, Fig. 3; Thompson 2000, Fig. 3). These external crystallites can be sloughed off or sedimented together with dead cells.

Evidence that Ca^{2+} adsorption is a key step in calcification comes from experimental studies that observed cyanobacteria to precipitate combinations of strontionite (SrCO_3), magnesite (MgCO_3) and mixed calcium-strontionite carbonates when grown in the presence of various combinations of Sr^{2+} , Mg^{2+} or Ca^{2+} (Schultze-Lam and Beveridge, 1994). In general, cyanobacteria are equally capable of incorporating Ca^{2+} or Sr^{2+} into carbonate mineral formation, yet Mg-containing precipitates are easily inhibited by the preferential binding of the other two cations. Other studies have documented that cyanobacteria can partition up to 1.0 wt% strontium in calcite (Ferris *et al.*, 1995). However, our understanding of calcium adsorption to cyanobacteria is complicated by the fact that they can present differing surfaces to the external environment. For instance, cyanobacteria with sheaths generally precipitate more calcium carbonate than those without sheaths. The mucilaginous sheath that envelops benthic calcified cyanobacteria is a structured form of EPS that can provide support, stability, and protection against physical damage, including ultraviolet radiation, dehydration and grazers. It also binds solutes and reduces the diffusion of carbonate ions (formed during photosynthesis) to the bulk milieu. Calcium carbonate may nucleate on the sheath surface and grow radially outwards, or it may nucleate within the sheath, leading to the sheath's impregnation with mineral material (Riding, 1977). In present-day examples sheath calcification ranges from isolated crystals (Pentecost, 1987, Fig. 1d), through a crystalline network (e.g. Friedmann 1979, Fig. 9), to a relatively solid tube of closely juxtaposed crystals (e.g. Couté and Bury, 1988, plate 2). These differences in

degree of calcification appear to relate to both environmental and biological controls. Post-mortem sheath degradation by bacteria has also been suggested to lead to calcification, but degraded sheaths are irregular in form and encrusted by carbonate to varying degrees. In contrast, fossils such as *Girvanella* exhibit regular tube morphology in which wall-thickness remains constant in individual specimens, suggesting *in vivo* sheath impregnation (Riding, 1977, 2006).

The overriding environmental control on cyanobacterial calcification appears to be aquatic saturation with respect to CaCO_3 minerals (Kempe and Kazmierczak, 1994). At the present-day this is reflected in the limitation of cyanobacterial sheath calcification to calcareous lakes and freshwater streams. A striking additional observation is that calcified cyanobacteria appear to be very rare in present-day marine environments, whereas sheath calcified microfossils were common in ancient shallow marine environments, especially during the Paleozoic and Mesozoic (Riding, 1982), suggesting a significant reduction in carbonate saturation. Similarly, biogenic whittings are well-known in some present-day calcareous lakes, and are inferred to have contributed a significant proportion of marine carbonate mud from the mid-Proterozoic to late Mesozoic; but their development in present-day marine environments, although strongly suspected, is not confirmed.

8.5.1.2 Sedimentary products

Biogenic whittings Small cyanobacteria ($<2\mu\text{m}$ in size), known as picoplankton, have long been linked to fine-grained calcium carbonate precipitation in the water column. These whiting events can occur in lakes during times of seasonal blooms and locally are responsible for the bulk of the sedimentary carbonate deposits. One well described site is Fayetteville Green Lake in New York State, where active growth of the unicellular cyanobacterium *Synechococcus* sp. during the summer months leads to calcite formation on the extracellular S-layers (Thompson *et al.*, 1990). Consequently, a light rain of calcite-encrusted plankton falls to the lake bottom each summer, contributing to unconsolidated carbonate mud deposition. Interestingly, during the cold winter months, when the *Synechococcus* cells become dormant, the non-metabolizing cells develop abundant gypsum ($\text{CaSO}_4 \cdot 2\text{H}_2\text{O}$) crystals on their S-layers instead of calcite – the formation of gypsum is the thermodynamically predictable phase given the high dissolved sulfate concentrations in the lake. Importantly, this ability to switch biominerals testifies to the lack of control exerted by the cyanobacteria in this biominerization process. The carbonate crystals are sedimented through the water column individually, or as poorly structured aggregates along with organic cells, to accumulate as

layers of carbonate mud on the lake bed, often in seasonally varved deposits (Kelts and Hsü, 1978).

There has been considerable debate regarding the origins of present-day marine 'whitings' on the Bahaman Banks. Satellite imagery has shown some whitings to cover as much as 200 km² during the summer (Shinn *et al.*, 1989) and it has been suggested that cyanobacterial whitings could account for much of the late Holocene bank-top lime muds on the Great Bahamas Bank (Robbins *et al.*, 1997). Field studies provided putative evidence in support of a microbial origin for the whitings due to the presence of 25% by weight organic matter in the solid whiting material and electron microscopy (SEM/TEM) images that showed individual whiting spheres embedded in an organic matrix, along with the presence of CaCO₃ crystals on cyanobacterial surfaces (Robbins and Blackwelder, 1992). However, whitings generally occur in very shallow water, and it is thus possible that they may also include a component of resuspended mud. This interpretation is supported by whiting CaCO₃ having a ¹⁴C/¹²C ratio different to that of inorganic carbon in the surrounding water (Broecker *et al.*, 2000). Consequently, re-suspension of sediment could be the dominant process involved in marine whitings on the Bahaman Banks (Broecker *et al.*, 2001).

Calcified sheaths At the present-day, calcified cyanobacteria are rare in normal marine environments, although they were common at many times in the past. This secular distribution most likely reflects the relatively low carbonate saturation state of present-day oceans. Consequently, information concerning calcified cyanobacteria has to be obtained from non-marine environments, and they are most common as tufa deposits in hardwater streams fed by springs in limestone areas. As it emerges, groundwater loses CO₂ to the atmosphere, increasing carbonate saturation, resulting in the precipitation of calcium carbonate on cyanobacterial sheaths. In fast flowing streams cyanobacterial photosynthesis may utilize CO₂ and calcification appears largely as a surface crust on the sheaths. In slower flowing streams and lakes, in contrast, the sheaths are impregnated by carbonate crystals, probably reflecting localized pH increase due to bicarbonate uptake (Merz-Preiß and Riding, 1999). These contrasting styles of calcification emphasize the large differences that can occur even within so-called 'biologically induced calcification'. Importantly, it is this sheath-induced calcification that creates microfossils, recognizable in marine environments back to at least the Mesoproterozoic (Kah and Riding, 2007). When well-preserved, these are morphologically simple but nonetheless distinctive. They include delicate tubes (e.g. *Girvanella* and *Ortonella*) and dendritic shrub-like masses (e.g. *Angusticellularia*) that

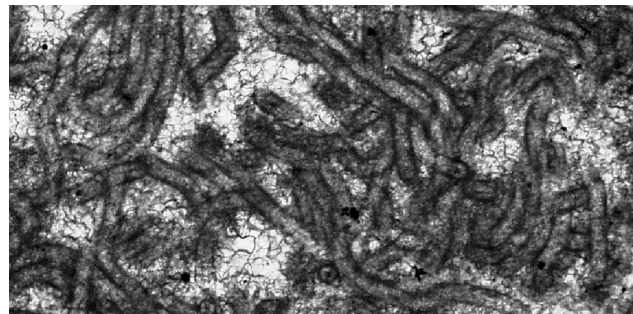


Figure 8.6 CaCO₃-impregnated cyanobacterial sheath preserved as the calcified microfossil *Girvanella*, early Mid-Ordovician, Lunnan, Tarim, China. Width of view 1 mm.

have present-day analogues in calcified filamentous cyanobacteria. In marine environments they typically accumulated *in situ* as components of stromatolites, oncoids, thrombolites, dendrolites, reef crusts, and other microbial mat deposits. Occasionally, however, they occurred as loosely tangled planktic or semi-planktic filaments as in some *Girvanella* (Fig. 8.6).

Tufa and travertine Aquatic mosses are often abundant and heavily calcified in tufa streams that channel the water flow. As in cyanobacteria, in these fast-flowing conditions it appears that calcification is not directly related to moss photosynthesis but instead is associated with a microbial biofilm growing on the moss that includes cyanobacteria and small algae (Freytet and Verrecchia, 1999; Pentecost, 2005). Moss and cyanobacterial tufas can create substantial barriers that block rivers, creating lakes between which water cascades over tufa dams. This localized turbulence and evaporation promotes degassing of CO₂ that enhances carbonate precipitation, providing a positive feedback to further tufa formation. Ultimately such barriers can fail or the water is diverted to other routes, but while they exist they can create spectacular natural water gardens, as at Plitvice in Croatia (Golubić *et al.*, 2008). In these environments the link between biofilms and calcification is suggested by experiments in which copper substrates toxic to microbes remain uncalcified (Srdoč *et al.*, 1985), whereas biofilms form on other substrates and calcify.

The organisms that create substrates for carbonate precipitation in ambient-water streams are responsible for the typically highly porous structure of tufa. In contrast, the chemistry and temperature of hot water springs promote even more rapid carbonate precipitation but tend to inhibit growth of all but the most hardy microorganisms. As a result, organic substrates are often inconspicuous and the resulting travertine deposit may be sinter-like (the siliceous precipitates associated with hot springs). There are complex intergradations between

tufa and travertine, but hot spring water is generally subject to such rapid increase in saturation that much of the carbonate is deposited very close to the springs in ridges or steep terraces such as Mammoth Hot Springs, in Yellowstone National Park, USA (Fouke *et al.*, 2000). These deposits appear to be essentially abiogenic, and the effect of microorganisms on their fabric is less than in the tufa of cool water streams (Pentecost, 2005). However, some distinctive travertine deposits such as dendritic shrub-like fabrics, have been regarded as the calcification products of bacteria other than cyanobacteria due to the presence of numerous micron-sized bodies interpreted as the remains of bacterial cells (Chafetz and Folk, 1984).

8.5.2 Bacteria

Bacteria other than cyanobacteria have long been suggested to contribute to the formation of a variety of non-skeletal sedimentary carbonates, including carbonate mud, ooids, clotted micrite fabrics, stromatolites, peloids, and peloidal cements. Drew (1913) proposed that abundant lime mud accumulating west of Andros Island on the Bahaman Banks, and in parts of the Florida Keys, is a bacterial precipitate, and also suggested that oolitic limestone may owe its origin to 'some diagenetic change in the precipitate of finely divided calcium carbonate particles produced in this way by bacterial action'. He and other early researchers (see Ehrlich, 2002) were impressed by the abundance of bacteria in carbonate sediments. They found that when grown under laboratory conditions, a wide variety of bacteria were able to precipitate carbonate minerals. The drawback to this approach lies in the differences between laboratory and field conditions, particularly with regard to aqueous chemistry, and growth media composition and consistency. Efforts continue to elucidate the effects of specific organic functional groups on carbonate morphology and mineralogy, e.g. spherule vs. euhedral calcite or calcite vs. aragonite (e.g. Braissant *et al.*, 2004), and also to explore links between bacterial activity and the formation of carbonate grains such as mud (e.g. Thompson, 2000) and ooids (e.g. Plée *et al.*, 2008). Particularly close attention has been paid to the development of stromatolitic microfabrics, such as clotted and peloidal micrite, in microbial mats.

8.5.2.1 Calcification mechanisms in microbial mats

Microbial mats are complex, densely populated algal-bacterial communities that develop on illuminated sediment surfaces that are intermittently or permanently water-covered (e.g. Revsbech *et al.*, 1983; van Gemerden, 1993). They have long been regarded as a key to understanding stromatolites (e.g. Walcott, 1914; Monty, 1976).

In shallow water, mat life is based on energy cycling between 'primary producers' that photosynthetically fix inorganic carbon, and 'decomposers' that efficiently recycle these organic products. In present-day marine mats the main primary producers of organic matter are cyanobacteria, whereas decomposers release energy from the organic matter by transferring electrons from the reduced carbon to available oxidants such as O_2 , NO_3^- , SO_4^{2-} , and CO_2 (see Konhauser, 2007, chapter 6). These processes can significantly change alkalinity and pH (Baas-Becking *et al.*, 1960), and thus, they affect carbonate precipitation and dissolution (Canfield and Raiswell, 1991b). For example, nitrate reduction 'recall reaction 8.14' and sulfate reduction (recall reaction 8.17) contribute to localized increases in HCO_3^- level, and therefore raised alkalinity, that can promote supersaturation with respect to calcium carbonate minerals (Visscher and Stoltz, 2005). This, in turn, can lead to the nucleation of fine-grained carbonates that entomb living and dead microorganisms in a lithified matrix (e.g. Castanier *et al.*, 2000). In an opposing manner, aerobic respiration in the surface mat promotes carbonate dissolution through the production of dissolved CO_2



Calcium-binding by EPS and its release during degradation, as well as the spatial separation of biological processes that affect carbonate dissolution and precipitation, contribute to significant local variations in carbonate precipitation within mats (Dupraz and Visscher, 2005).

8.5.2.2 Sedimentary products: stromatolites

The characteristic feature of stromatolites is lamination that reflects episodic but relatively evenly distributed accretion associated with microbial growth and calcification, and locally also with abiogenic precipitation and grain trapping. Their record commences 3.5 Ga. By contrast, thrombolites are microbial carbonates with a macroscopically clotted fabric (Aitken, 1967). They first appeared in abundance in the mid-Proterozoic, concurrent with the presence of recognizable calcified cyanobacterial filaments in the rock record, and were particularly common in the Cambrian and Early Ordovician. Present-day thrombolites that are strikingly similar in appearance to Early Palaeozoic examples form through cyanobacterial calcification in the marginal marine Lake Clifton in Western Australia (Moore and Burne, 1994), but thrombolitic fabrics are also associated with laminated fabrics in Shark Bay (Aitken, 1967) and Lee Stocking columns (Feldmann and McKenzie, 1998) that mainly form by trapping and binding sandy carbonate sediment, together with episodic lithification (Reid *et al.*, 2000). Thrombolites therefore

appear to have a variety of origins, and – unlike stromatolites – have the additional distinction that their characteristic clotted appearance can be significantly enhanced by diagenetic alteration.

Although some stromatolite-like deposits may be essentially abiogenic seafloor crusts (e.g. Grotzinger and Rothman, 1996; Riding, 2008), many stromatolites, especially Phanerozoic examples, can confidently be interpreted as lithified microbial mats (Chapter 16). Present-day calcified shallow-water mats, formed by communities of cyanobacteria and other bacteria, have complex fabrics comparable with those of many Phanerozoic and also Proterozoic stromatolites. They can include well-defined microfossils such as calcified cyanobacterial sheaths, but these are generally volumetrically subordinate to fine-grained clotted and peloidal carbonate microfabrics that mostly represent the synsedimentary calcification of bacterial cells and cell products. The peloids are irregular micritic aggregates commonly 20–60 microns in size. Both clotted texture and associated peloids have been linked to bacterial calcification in general, and sulfate reduction in particular (Pigott and Land, 1986; Chafetz 1986; Heindel *et al.*, 2010). Formation of these microfabrics during degradation of organic matter, that includes bacterial cell wall material, EPS and other organic macromolecules, helps to explain their complexity (see Riding, 2000; Dupraz and Visscher, 2005).

8.5.2.3 Dolomitization

The experimental abiotic formation of dolomite $[CaMg(CO_3)_2]$ at low temperatures is difficult, if not impossible, even from supersaturated solutions. In contrast, in nature dolomite commonly has been reported as an early replacement mineral of calcite and/or aragonite. Again, it has been realized that bacterial sulfate reduction can be directly involved because it overcomes the kinetic barrier to dolomite formation by increasing the pH and alkalinity, and removes sulfate which is a known inhibitor to dolomite formation (Baker and Kastner, 1981; Lyons *et al.*, 1984; van Lith *et al.*, 2003a). The environments from which bacterial dolomite has been reported range from deep marine (Friedman and Murata, 1979) to shallow hypersaline lagoons (Gunatilaka *et al.*, 1984). Since sulfate occurs in seawater as a magnesium-sulfate ion pair, its removal also increases magnesium availability for dolomite precipitation in the microenvironment around the cell (Van Lith *et al.*, 2003b). Furthermore, sulfate-reducing bacteria have been shown to experimentally precipitate dolomite crystals identical in composition and morphology to those found in the natural systems where the bacteria were isolated (Warthmann *et al.*, 2000).

Dolomite has also been shown to form in basalt-hosted aquifers, in association with methanogenic bac-

teria (Roberts *et al.*, 2004). Dissolution of basalt yields elevated pore-water concentrations of dissolved Ca^{2+} and Mg^{2+} , which can adsorb onto cell surfaces. Together with the methanogenic consumption of CO_2 that generates alkalinity, this locally increases carbonate saturation and results in the formation of small dolomite grains (10s of nanometers in diameter) directly on the cell surfaces, and at times, completely encrusting them (Kenward *et al.*, 2009).

8.5.3 Geological implications

It can be expected that bacterial calcification should have responded to long-term variations in atmosphere-hydrosphere composition because these global changes would have affected carbonate saturation and bacterial metabolism (e.g. sulfate reduction, photosynthesis). Indeed, there is evidence that these changes may be reflected in the secular abundance of bacterial carbonates, and in the fabrics developed by stromatolites and other microbial carbonates (Fig. 8.7).

8.5.3.1 Stromatolites

Microbial mat fabrics developed in association with precipitated abiogenic crusts during the Archean and early-mid Proterozoic (Sumner, 1997). This is also suggested by the regular and even laminations common in these stromatolites, and by the alternating dark (fine-grained) and light (sparry) layers of which some of them consist (Riding, 2008). As abiogenic precipitation declined and lithified microbial mats increased over time, marine stromatolites developed the uneven layering and dominantly fine-grained, clotted-peloidal fabrics that characterize many Phanerozoic examples. During the Proterozoic, reduction in abiogenic precipitation probably reflects a general decline in seawater carbonate saturation (Grotzinger, 1990) and the development of clotted-peloidal fabrics may relate to increased levels of seawater sulfate that promoted bacterial sulfate reduction. The mid-Proterozoic appearance of calcification of cyanobacterial sheaths could indicate that decline in atmospheric CO_2 had reached a critical threshold stimulating cyanobacteria to develop CCMs (Riding, 2006). In this view, the development of the clotted/peloidal (spongistrome) and tubiform (porostromate) microfabrics that are widespread in lithified microbial mats during the Phanerozoic were the respective products of bacterial sulfate reduction and cyanobacterial CCM development. In addition, it seems likely that calcified cyanobacteria complicated and coarsened microbial carbonate macrofabrics sufficiently to give them a dominantly clotted rather than laminated appearance, and thrombolites were born.

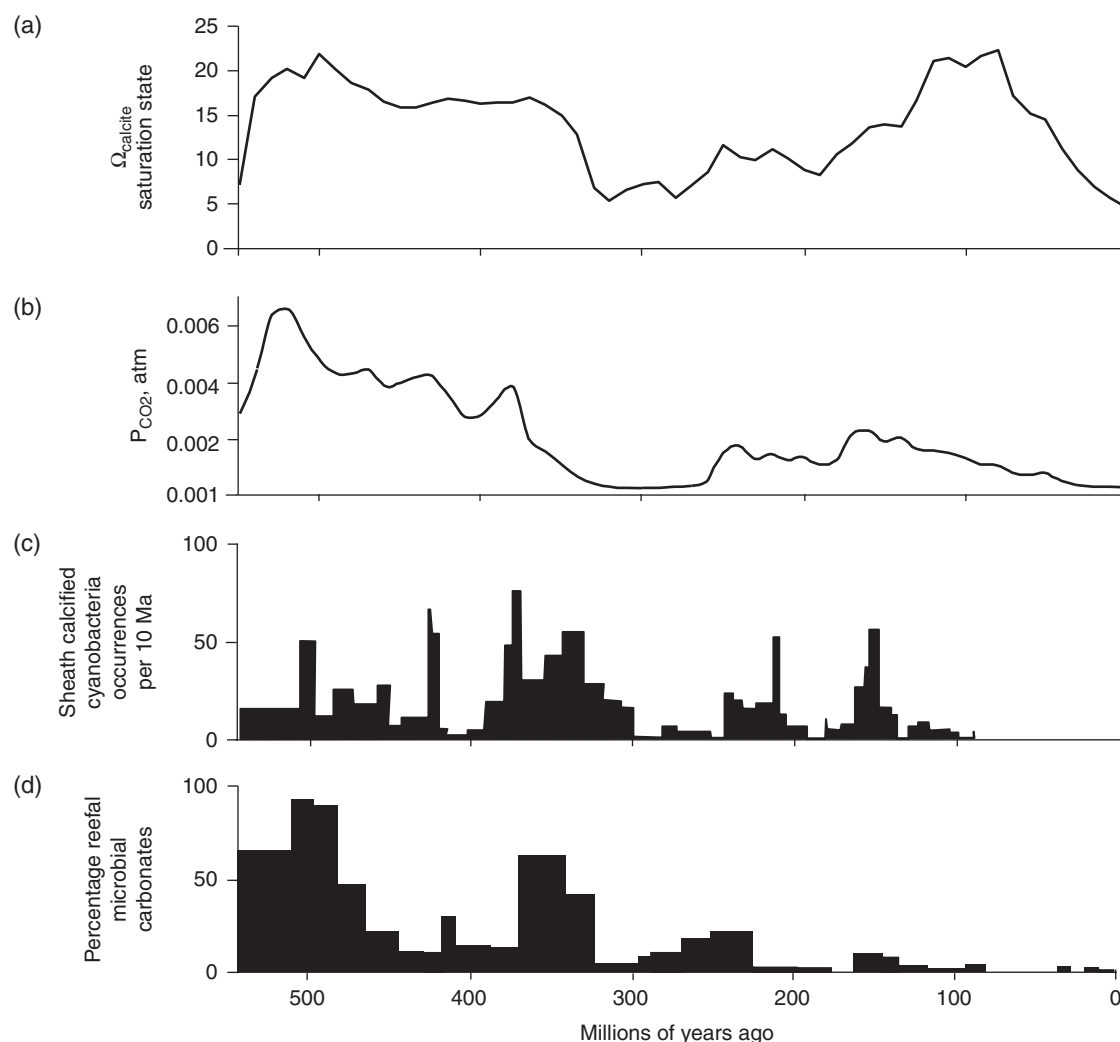


Figure 8.7 Phanerozoic trends of (a) seawater calcite saturation state (Ω_{calcite}) (Riding and Liang 2005b, Fig. 5), (b) atmospheric CO_2 (Berner and Kothavala, 2001, Fig. 13 GEOCARB III), (c) marine calcified cyanobacteria occurrences (Arp *et al.*, 2001, Fig. 3d), (d) reefal microbial abundance (Kiessling, 2002, Fig. 16).

Long-term decline in the abundance of microbial carbonates, such as stromatolites, has often been attributed to both eukaryote competition and reduction in carbonate saturation state (Fischer, 1965), although the inception of this decline before the appearance of metazoans suggests the latter as the major influence (Grotzinger, 1990). This, together with a lower rate of microbial growth, could also have affected stromatolite morphology, since the external shapes of stromatolites are significantly determined by the accretion rate relative to adjacent sediment (Riding, 1993). Low relative accretion rate results in low relief, making stromatolites more prone to lateral incursion by sediment, and fostering complex shapes, such as digitate forms. In contrast, high relative accretion rates promote high relief and simple shapes, such as domes and cones. Consequently, although mid-Proterozoic increase in

morphotypic diversity (e.g. in branched stromatolites), has been regarded as a proxy for abundance, it could be that complex shape reflects low synoptic relief due to reduced relative accretion rate. If so, then it might be a sign that stromatolite growth was in decline. The Phanerozoic is characterized by episodic development of dendrolites and thrombolites, for example in the Cambro-Ordovician and Late Devonian, and also by changes in microbial carbonate abundance in general. These patterns may reflect broad positive correspondence between reefal microbial carbonate abundance (Kiessling, 2002, see their Fig. 16) and calculated seawater saturation state for CaCO_3 minerals during much of the Palaeozoic and Mesozoic (Riding and Liang, 2005a) (Fig. 8.7a,d). Breakdown in this pattern ~120–80 Ma ago (when the calculated saturation ratio was high but microbial carbonate abundance was low) could reflect

removal of carbonate deposition by pelagic plankton that significantly reduced the actual saturation state.

Nonetheless, the important influence of saturation state on stromatolite accretion and preservation does not preclude significant additional long-term effects on stromatolite and thrombolite development as a result of eukaryote evolution. It is debatable whether metazoan grazing significantly affected stromatolite development so long as carbonate saturation was high enough to ensure microbial mat lithification, but overgrowth by skeletonized algae and invertebrates must have inhibited the formation of well-defined microbial structures from the mid-Ordovician onwards. As a result, microbial carbonates were subsumed within complex reef structures where, lacking space to form domes and columns, they developed as patchy and irregular crusts on and around skeletal organisms. This made them appear much less abundant than they really were (Pratt, 1982). Exceptions to this pattern could have occurred in the immediate aftermaths of mass extinction events that killed skeletal reef builders, and also in ecological refuges such as at present-day Shark Bay (Logan, 1961) and Lee Stocking Island (Dill *et al.*, 1986). In these situations, unconstrained by algal and invertebrate reef organisms, microbial mats were once again able to develop distinctive morphologies, including metric scale steep sided columns.

Uncalcified algae also transformed mat communities. For example, diatoms and green algae are abundant in Shark Bay (Awramik and Riding, 1988) and Lee Stocking (Riding *et al.*, 1991) mats and confer added ability to trap sediment that can be much larger (sand, gravel) than in most ancient stromatolites. This creates coarse and crudely layered fabrics that are locally thrombolitic. Thus, these examples of present-day columns reflect the combination of at least two favourable factors: the trapping abilities of both cyanobacteria and algae, and salinity and current stressed conditions that inhibit overgrowth by reef organisms. The first of these promotes rapid accretion, while the second hinders disruption of the microbial mats. Overall, however, marine microbial carbonates are scarcer today than at almost any other time during the Phanerozoic. Presumably this reflects at least two present-day conditions: the abundance of skeletal reef builders, and relatively low carbonate saturation state.

8.5.3.2 Calcified cyanobacteria

The earliest record of cyanobacterial calcification is from the early Proterozoic (Klein *et al.*, 1987), although sheath-calcified cyanobacteria seem to be remarkably scarce until ~1.2 Ga (Kah and Riding, 2007) and they only became widespread in the Neoproterozoic. They remained locally very common in shallow marine carbonates throughout much of the Palaeozoic and

Mesozoic, but then became scarce by the mid-Cretaceous and are rare in present-day normal marine environments (Riding, 1982; Arp *et al.*, 2001). This unusual secular distribution is hypothesized to be due to the combined effects of CCM induction (and therefore changes in atmospheric CO₂) and fluctuations in carbonate saturation state (Riding, 2006).

Badger *et al.* (2002) proposed that cyanobacterial CCMs developed in the Late Palaeozoic in response to both CO₂ decline and O₂ increase. However, similarly large changes in CO₂ levels are thought to have occurred in the mid-Proterozoic (Kasting, 1987), and it has been suggested that cyanobacterial CCMs first developed then, coincident with the appearance of calcified sheath microfossils (Riding, 2006; Kah and Riding, 2007). The reasoning is that under high early Proterozoic CO₂ levels, cyanobacterial photosynthesis would have relied on CO₂ diffusion that would not have significantly altered pH near the cells. As atmospheric CO₂ level fell in the mid-Proterozoic, cyanobacteria began to pump in bicarbonate to maintain photosynthesis, and the conversion of bicarbonate to CO₂ resulted in OH⁻ production that raised pH, stimulating calcification (see Section 8.5.1.1). Thus, cyanobacterial CCM development promoted sheath calcification and whiting production. Appearance of sheath-calcified microfossils ~1.2 Ga ago could therefore reflect reduction in atmospheric CO₂ level below the threshold of ~0.36% (~10 times the present preindustrial atmospheric level) at which cyanobacteria induce CCMs in experiments (see Badger *et al.*, 2002; Riding, 2006).

During much of the Palaeozoic and Mesozoic, fluctuations in calcified sheath abundance (Arp *et al.*, 2001) and also reefal microbial carbonate abundance (Kiessling, 2002, Fig. 16) broadly track some estimates of seawater carbonate saturation (Riding and Liang, 2005b) (Figure 8.8). The abundance of sheath calcified cyanobacteria when CO₂ levels are thought to have been high (see Berner and Kothavala, 2001), e.g. during the early-mid Palaeozoic, suggests that CCMs continued to be induced even when p_{CO₂} substantially exceeded 10 PAL. This could be because calcified sheaths developed in microbial mat and reef environments where cyanobacteria experienced localized carbon limitation that necessitated CCM activation (Riding, 2006). The broader influence of p_{CO₂} on CCMs may be reflected in the Mississippian, when calcified sheath abundance increased as p_{CO₂} declined (Riding, 2006, 2009).

As noted with regard to reefal microbial carbonates, reduction in sheath calcified cyanobacteria ~120–80 Ma ago could reflect reduction in actual (as opposed to calculated) saturation state resulting from the burial of abundant carbonate precipitated as calcified skeletons by plankton such as coccolithophore algae and globigerine foraminifers (Riding and Liang, 2005a), and this effect may have continued into the Palaeogene. Since the

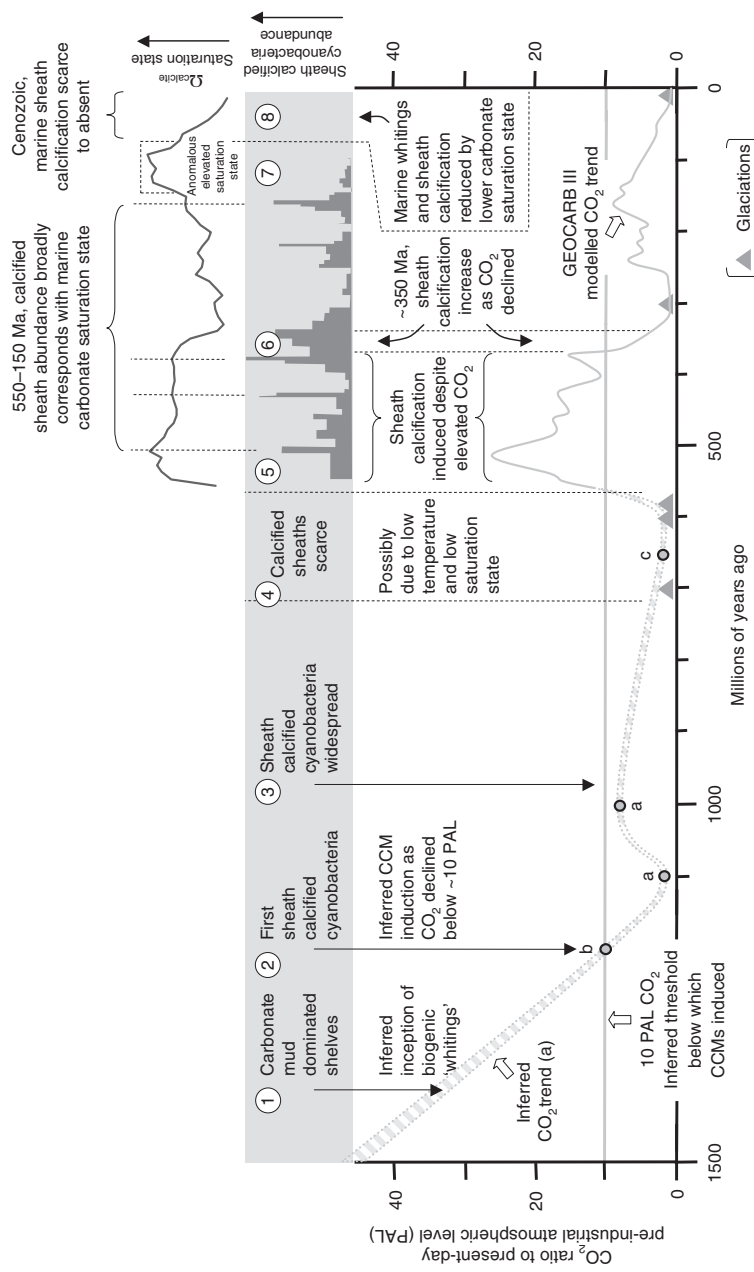


Figure 8.8 Conjectural history of cyanobacterial marine sheath calcification and picoplanktic 'whiting' precipitation. The Proterozoic inferred CO_2 trend is based on (a) Sheldon (2006), (b) Kah and Riding (2007), (c) Hyde *et al.* (2000) and (d) Ridgwell *et al.* (2003); the continuous trend line is from Berner & Kothavala (2001, fig. 13); the Neoproterozoic glaciations is from Walter *et al.* (2000); the occurrences of marine sheath calcified cyanobacteria is from Arp *et al.* (2001, fig. 3d); the calculated carbonate saturation states are from Riding and Liang (2005b, fig. 5); and the threshold below which CCMs are induced is based on Badger *et al.* (2002). Several key developments can be inferred from the figure. (1) Photosynthetic 'whitenings', as reflected by widespread carbonate mud sedimentation, may have been triggered as CO_2 reduced pH buffering (see Arp *et al.*, 2001; Riding, 2006). (2) A further decline below ~10 PAL CO_2 induced CCM development and sheath calcification at ~1200 Ma (Kah and Riding, 2007). (3) Calcified sheaths were widespread in the early Neoproterozoic (see references in Knoll and Semikhatov 1998), but (4) became scarce during 'Snowball' glaciations, possibly due to reduction in CCM development as low temperatures favoured diffusive entry of CO_2 into cells, and due to lower seawater saturation state reflecting reduction in both temperature and p_{CO_2} . (5) Sheath calcification was common in marine environments during the early-mid Palaeozoic despite elevated CO_2 , suggesting that once CCMs had developed they were readily induced where carbon limitation developed, such as microbial mats. Throughout much of the Palaeozoic and early Mesozoic, calcified sheath abundance appears to vary with carbonate saturation state. (6) As CO_2 declined in the Late Devonian-Early Mississippian, calcified sheath abundance temporarily increased, possibly reflecting enhanced CCM induction, but then declined as the saturation state dropped in the Mississippian-Pennsylvanian (Riding, 2009). (7) Despite a high calculated saturation state in the Late Cretaceous-Palaeogene, planktic calcifiers probably reduced the actual saturation state sufficiently to inhibit cyanobacterial calcification. Thus, calcified sheaths were scarce in marine environments. (8) Since the Eocene, low carbonate saturation – due to low levels of both Ca ions and pCO_2 – is reflected in extreme scarcity in sheath calcification in marine environments.

Eocene, under the influence of low levels of Ca^{2+} ions and p_{CO_2} , seawater carbonate saturation was reduced to a Phanerozoic low only matched in the Late Palaeozoic (Riding and Liang, 2005a; see their Fig. 5a). Consequently, despite low p_{CO_2} values during the Cenozoic (see Berner and Kothavala, 2001) that would have induced cyanobacterial CCMs, sheath calcification has not been observed in marine cyanobacteria, and this presumably reflects low carbonate saturation.

8.5.3.3 Biogenic whitings

It has been widely supposed that a significant proportion of Proterozoic carbonate mud may have derived from 'whitings' stimulated by photosynthetic CO_2 uptake by photosynthetic phytoplankton (Grotzinger, 1989, 1990). Through much of the Proterozoic, carbonate mud abundance appears to exhibit a first order trend of increase with decreasing age. Absence of carbonate mud in the Late Archaean (Sumner and Grotzinger, 2004) and scarcity in the Palaeoproterozoic (e.g. Kah and Grotzinger, 1992), was followed by an increase that transformed cement-rimmed platform margins into muddy carbonate ramps ~ 1.4 – 1.3 Ga (Sherman *et al.*, 2000, p. 290). By the early Neoproterozoic, both calcified cyanobacteria (Swett and Knoll 1985; Knoll and Semikhatov, 1998) and carbonate mud accumulation (Herrington and Fairchild, 1989) were widespread. It can be postulated that this transition to carbonate mud dominated platforms reflects inception of whiting precipitation as p_{CO_2} declined and CCMs developed in cyanobacteria (Riding, 2006).

Since CCMs promote bloom conditions by conferring ability to overcome carbon limitation (Rost *et al.*, 2003), CCM-stimulated picoplanktic mud production on carbonate shelves may have continued to exert a major influence on subsequent carbonate sedimentation whenever carbonate saturation state was sufficiently elevated, for example, during the early-mid Palaeozoic and parts of the Mesozoic. These biogenic whitings should have been further intensified whenever p_{CO_2} levels fell to levels near or below ~ 10 present atmospheric levels. Eventually, as seawater carbonate saturation levels declined in the Cenozoic this process should have slowed, despite falling p_{CO_2} . Thus, as noted above (Section 8.5.1.2), it has been suggested that present-day marine 'whitings' on the Bahama Banks could be biogenic (Robbins and Blackwelder, 1992), but may dominantly be formed by sediment resuspension (Broecker *et al.*, 2000). If present-day biogenic marine whitings produced by cyanobacteria are in fact scarce, it most likely reflects relatively low present-day levels of seawater carbonate saturation.

Bacterial calcification, strongly susceptible to environmental influence, is therefore a sensitive indicator of

changes in atmospheric and seawater composition over long geological time-scales. The fabrics of benthic bacterial carbonates such as stromatolites and thrombolites, and also their abundance together with that of bacterial whitings, have altered significantly during the Precambrian and Phanerozoic. Relating these developments to both environmental change and bacterial metabolic evolution offers fruitful areas for further research.

Acknowledgements

We express our appreciation to Tanja Bosak and Linda Kah for their detailed and useful suggestions.

References

- Aitken JD (1967) Classification and environmental significance of cryptalgal limestones and dolomites, with illustrations from the Cambrian and Ordovician of southwestern Alberta. *Journal of Sedimentary Petrology* **37**, 1163–1178.
- Alt JC (1988) Hydrothermal oxide and nontronite deposits on seamounts in the Eastern Pacific. *Marine Geology* **81**, 227–239.
- Altermann W, Schopf JW (1995) Microfossils from the Neoproterozoic Campbell Group, Crumland West Sequence of the Transvaal Supergroup, and their palaeoenvironmental and evolutionary implications. *Precambrian Research* **75**, 65–90.
- Arp G, Reimer A, Reitner J (2001) Photosynthesis-induced biofilm calcification and calcium concentrations in Phanerozoic oceans. *Science* **292**, 1701–1704.
- Awramik SM, Riding R (1988) Role of algal eukaryotes in subtidal columnar stromatolite formation. *Proceedings of the National Academy of Sciences, USA* **85**, 1327–1329.
- Baas-Becking LGM, Kaplan IR, Moore D (1960) Limits of the natural environment in terms of pH and oxidation-reduction potentials. *Journal of Geology* **68**, 243–284.
- Badger M, Price D (2003) CO_2 concentrating mechanisms in cyanobacteria: molecular components, their diversity and evolution. *Journal of Experimental Botany* **54**, 609–622.
- Badger MR, Hanson D, Price GD (2002) Evolution and diversity of CO_2 concentrating mechanisms in cyanobacteria. *Functional Plant Biology* **29**, 161–173.
- Baker PA, Kastner M (1981) Constraints on the formation of sedimentary dolomite. *Science* **213**, 214–216.
- Bekker A, Slack JF, Planavsky N, *et al.* (2010) Iron formation: a sedimentary product of the complex interplay among mantle, tectonic, and biospheric processes. *Economic Geology*, in press.
- Berner RA (1984) Sedimentary pyrite formation: an update. *Geochimica et Cosmochimica Acta* **48**, 605–615.
- Berner RA, Kothavala Z (2001) GEOCARB III. A revised model of atmospheric CO_2 over Phanerozoic time. *American Journal of Science* **301**, 182–204.
- Beveridge TJ (1984) Mechanisms of the binding of metallic ions to bacterial walls and the possible impact on microbial ecology. In: *Current Perspectives in Microbial Ecology* (eds Reddy CA, Klug MJ). American Society for Microbiology, Washington, DC, pp. 601–607.

- Beveridge TJ, Murray RGE (1976) Uptake and retention of metals by cell walls of *Bacillus subtilis*. *Journal of Bacteriology* **127**, 1502–1518.
- Bjerrum CJ, Canfield DE (2002) Ocean productivity before about 1.9 Gyr limited by phosphorous adsorption onto iron oxides. *Nature* **417**, 159–162.
- Blothe M, Roden, EE (2009) Composition and activity of an autotrophic Fe(II)-oxidizing, nitrate-reducing enrichment culture. *Applied and Environmental Microbiology* **75**, 6937–6940.
- Braissant O, Cailneau G, Aragno M, Verrecchia EP (2004) Biologically induced mineralization in the tree *Milicia excelsa* (Moraceae): its causes and consequences to the environment. *Geobiology* **2**, 59–66.
- Brocks JJ, Logan GA, Buick R, Summons RE (1999) Archean molecular fossils and the early rise of eukaryotes. *Science* **285**, 1033–1036.
- Broecker WS, Sanyal A, Takahashi T (2000) The origin of Bahamian whittings revisited. *Geophysical Research Letters* **27**, 3759–3760.
- Broecker WS, Langdon C, Takahashi T, Peng TH (2001) Factors controlling the rate of CaCO₃ precipitation on the Great Bahama Bank. *Global Biogeochemical Cycles* **15**, 589–596.
- Bosak T, Greene SE, Newman DK (2007) A possible role for anoxygenic photosynthetic microbes in the formation of ancient stromatolites. *Geobiology* **5**, 119–126.
- Buick R (1992) The antiquity of oxygenic photosynthesis: evidence for stromatolites in sulphate-deficient Archaean lakes. *Science* **255**, 74–77.
- Canfield DE, Raiswell R (1991a) Pyrite formation and fossil preservation. In: *Taphonomy: Releasing the Data Locked in the Fossil Record* (eds Allison PA, Briggs DEG). Plenum Press, New York, pp. 337–387.
- Canfield DE, Raiswell R (1991b) Carbonate precipitation and dissolution. In: *Taphonomy: Releasing the Data Locked in the Fossil Record* (eds Allison PSA, Briggs DEG). Plenum Press, New York, pp. 411–453.
- Castanier S, Le Métayer-Levrel G, Perthuisot J-P (2000) Bacterial roles in the precipitation of carbonate minerals. In: *Microbial Sediments* (eds Riding R, Awramik SM). Springer-Verlag, Berlin, Germany, pp. 32–39.
- Chafetz HS (1986) Marine peloids: a product of bacterially induced precipitation of calcite. *Journal of Sedimentary Petrology* **56**, 812–817.
- Chafetz HS, Folk RL (1984) Travertines: depositional morphology and the bacterially constructed constituents. *Journal of Sedimentary Petrology* **54**, 289–316.
- Cloud PE (1965) Significance of the Gunflint (Precambrian) microflora. *Science* **148**, 27–35.
- Cloud PE (1973) Paleoecological significance of the banded iron-formation. *Economic Geology* **68**, 1135–1143.
- Coleman ML (1985) Geochemistry of diagenetic non-silicate minerals. Kinetic considerations. *Philosophical Transactions of the Royal Society of London* **315**, 39–56.
- Couté A, Bury E (1988) Ultrastructure d'une Cyanophycée aérienne calcifère cavernicole: scytoneuma julianum Frank (Richter) (Hormogonophidiae, Nostocales, Scytonemataceae). *Hydrobiologia* **160**, 219–239.
- Cowen JP, Massoth GJ, Baker ET (1986) Bacterial scavenging of Mn and Fe in a mid- to far-field hydrothermal particle plume. *Nature* **322**, 169–171.
- Dill RF, Shinn EA, Jones AT, Kelly K, Steinen RP (1986) Giant subtidal stromatolites forming in normal salinity waters. *Nature* **324**, 55–58.
- Drew GH (1913) On the precipitation of calcium carbonate in the sea by marine bacteria, and on the action of denitrifying bacteria in tropical and temperate seas. *Journal of the Marine Biological Association* **9**, 479–524.
- D'Hondt S, Rutherford S, Spivack AJ (2002) Metabolic activity of subsurface life in deep-sea sediments. *Science* **295**, 2067–2070.
- Dupraz C, Visscher PT (2005) Microbial lithification in marine stromatolites and hypersaline mats. *Trends in Microbiology* **13**, 429–438.
- Dzombak DA, Morel FMM (1990) *Surface Complexation Modeling. Hydrous Ferric Oxide*. John Wiley & Sons, Inc., New York.
- Edwards KJ, Rogers DR, Wirsén CO, et al. (2003) Isolation and characterization of novel psychrophilic, neutrophilic, Fe-oxidizing, chemolithoautotrophic – Proteobacteria from the deep sea. *Applied and Environmental Microbiology* **69**, 2906–2913.
- Ehrenreich A, Widdel F (1994) Anaerobic oxidation of ferrous iron by purple bacteria, a new type of phototrophic metabolism. *Applied and Environmental Microbiology*, **60**, 4517–4526.
- Ehrlich HL (2002) *Geomicrobiology*, 4th edn. Marcel Dekker, New York, 768pp.
- Eigenbrode JL, Freeman KH (2006) Late Archean rise of aerobic microbial ecosystems. *Proceedings of the National Academy of Sciences, USA*, **103**, 15759–15764.
- Emerson D (2000) Microbial oxidation of Fe(II) and Mn(II) at circumneutral pH. In: *Environmental Microbe-Metal Interactions* (ed Lovley DR). ASM Press, Washington, DC, pp. 31–52.
- Emerson D, Moyer CL (2002) Neutrophilic Fe-oxidizing bacteria are abundant at the Loihi Seamount hydrothermal vents and play a major role in Fe oxide deposition. *Applied and Environmental Microbiology* **68**, 3085–3093.
- Emerson D, Revsbech NP (1994a) Investigation of an iron-oxidizing microbial mat community located near Aarhus, Denmark. Field studies. *Applied and Environmental Microbiology* **60**, 4022–4031.
- Emerson D, Revsbech NP (1994b) Investigation of an iron-oxidizing microbial mat community located near Aarhus, Denmark: laboratory studies. *Applied and Environmental Microbiology* **60**, 4032–4038.
- Emerson D, Fleming EJ, McBeth JM (2010) Iron-oxidizing bacteria: an environmental and genomic perspective. *Annual Reviews in Microbiology* **64**, 561–583.
- Feldmann M, McKenzie JA (1998) Stromatolite-thrombolite associations in a modern environment, Lee Stocking Island, Bahamas. *Palaeos* **13**, 201–212.
- Ferris FG, Fratton CM, Gerits JP, Schultze-Lam S, Sherwood Lollar B (1995) Microbial precipitation of a strontium carbonate phase at a groundwater discharge zone near Rock Creek, British Columbia, Canada. *Geomicrobiology Journal* **13**, 57–67.
- Ferris FG, Konhauser KO, Lyvén B, Pedersen K (1999) Accumulation of metals by bacteriogenic iron oxides in a subterranean environment. *Geomicrobiology Journal* **16**, 181–192.
- Fischer AG (1965) Fossils, early life, and atmospheric history. *Proceedings of the National Academy of Sciences, USA* **53**, 1205–1215.

- Fouke BW, Farmer JD, Des Marais DJ, et al. (2000) Depositional facies and aqueous-solid geochemistry of travertine-depositing hot springs (Angel Terrace, Mammoth Hot Springs, Yellowstone National Park, USA). *Journal of Sedimentary Research* **70**, 565–585.
- Fowle DA, Fein JB (2001) Quantifying the effects of *Bacillus subtilis* cell walls on the precipitation of copper hydroxide from aqueous solution. *Geomicrobiology Journal* **18**, 77–91.
- Freytet P, Verrecchia EP (1999) Calcitic radial palisadic fabric in freshwater stromatolites: diagenetic and recrystallized feature or physicochemical sinter crust? *Sedimentary Geology* **126**, 97–102.
- Friedmann EI (1979) The genus Geitleria (Cyanophyceae or Cyanobacteria): distribution of *G. calcarea* and *G. floridana* n. sp. *Plant Systematics and Evolution* **131**, 169–178.
- Friedman I, Murata KJ (1979) Origin of dolomite in Miocene Monterey Shale and related formations in the Temblor Range, California. *Geochimica et Cosmochimica Acta* **43**, 1357–1365.
- Ghiorse WC (1984) Biology of iron- and manganese-depositing bacteria. *Annual Reviews in Microbiology* **38**, 515–550.
- Ghiorse WC, Ehrlich HL (1992) Microbial biominerization of iron and manganese. In: *Biomineralization Processes* (eds Skinner HCW, Fitzpatrick RW). Catena Supplement, Cremlingen, Germany, pp. 75–99.
- Glasauer S, Langley S, Beveridge TJ (2001) Sorption of Fe hydr(oxides) to the surface of *Shewanella putrefaciens*: cell-bound fine-grained minerals are not always formed de novo. *Applied and Environmental Microbiology* **67**, 5544–5550.
- Golubić S (1973) The relationship between blue-green algae and carbonate deposits. In: *The Biology of Blue-Green Algae* (eds Carr NG, Whitton BA). Botanical Monographs **9**, Blackwell, Oxford, pp. 434–472.
- Golubić S., Violante C, Plenković-Moraj A, and Grgasović T. (2008). Travertines and calcareous tufa deposits: an insight into diagenesis. *Geologia Croatica* **61**, 363–378.
- Grotzinger JP (1989) Facies and evolution of Precambrian carbonate depositional systems. The emergence of the modern platform archetype. In: *Controls on Carbonate Platform and Basin Development* (eds Crevello PD, Wilson JL, Sarg JF). SEPM Special Publication, No. 44, Tulsa, OK, pp. 79–106.
- Grotzinger JP (1990) Geochemical model for Proterozoic stromatolite decline. *American Journal of Science* **290**, 80–103.
- Grotzinger JP, Rothman DR (1996) An abiotic model for stromatolite morphogenesis. *Nature* **383**, 423–425.
- Gunatilaka A, Saleh A, Al-Temeemi A, Nassar N (1984) Occurrence of subtidal dolomite in a hypersaline lagoon, Kuwait. *Nature* **311**, 450–452.
- Hafenbradl D, Keller M, Dirmeier R, et al. (1996) Ferroglobus placidus gen. nov., sp. nov., a novel hyperthermophilic archaeum that oxidizes Fe²⁺ at neutral pH under anoxic conditions. *Archives of Microbiology* **166**, 308–314.
- Hartman H (1984) The evolution of photosynthesis and microbial mats: a speculation on banded iron formations. In: *Microbial Mats: Stromatolites* (eds Cohen Y, Castenholz RW, Halvorson HO). Alan R. Liss, New York, pp. 451–453.
- Hayes JM (1983) Geochemical evidence bearing on the origin of aerobiosis, a speculative hypothesis. In: *Earth's Earliest Biosphere, Its Origin and Evolution* (ed Schopf JW). Princeton University Press, Princeton, NJ, pp. 291–301.
- Hegler F, Posth NR, Jiang J, Kappler A (2008) Physiology of phototrophic iron(II)-oxidizing bacteria—implications for modern and ancient environments. *FEMS Microbiology Ecology* **66**, 250–269.
- Heindel K, Birgel D, Peckmann J, Kuhnert H, Westphal H (2010) Formation of deglacial microbialites in coral reefs off Tahiti (IODP 310) involving sulfate-reducing bacteria. *Palaeos* **25**, 618–635.
- Heising S, Schink B (1998) Phototrophic oxidation of ferrous iron by a *Rhodomicromium vannielii* strain. *Microbiology* **144**, 2263–2269.
- Herrington PM, Fairchild IJ (1989) Carbonate shelf and slope facies evolution prior to Vendian glaciation, central East Greenland. In: *The Caledonide Geology of Scandinavia* (ed. Gayer RA). Graham and Trotman, London, UK, pp. 263–273.
- Holland HD (1973) The oceans: a possible source of iron in iron-formations. *Economic Geology* **68**, 1169–1172.
- Holm NG (1987) Possible biological origin of banded iron-formations from hydrothermal solutions. *Origin of Life* **17**, 229–250.
- Holm NG (1989) The 13C/12C ratios of siderite and organic matter of a modern metalliferous hydrothermal sediment and their implications for banded iron formations. *Chemical Geology* **77**, 41–45.
- Hyde WT, Crowley TJ, Baum SK, Peltier WR (2000) Neoproterozoic 'snowball Earth' simulations with a coupled climate/ice-sheet model. *Nature* **405**, 425–429.
- Irwin H, Curtis C, Coleman M (1977) Isotopic evidence for source of diagenetic carbonates formed during burial of organic-rich sediments. *Nature* **269**, 209–213.
- Ivarson KC, Sojak M (1978) Microorganisms and ochre deposits in field drains of Ontario. *Canadian Journal of Soil Science* **58**, 1–17.
- Jiao Y, Newman DK (2007) The pio operon is essential for phototrophic Fe(II) oxidation 521 in *Rhodopseudomonas palustris* TIE-1. *Journal of Bacteriology* **189**, 1765–1773.
- Juniper SK, Tebo BM (1995) Microbe–metal interactions and mineral deposition at hydrothermal vents. In: *The Microbiology of Deep-Sea Hydrothermal Vents* (ed. Karl DM). CRC Press, Boca Raton, FL, pp. 219–253.
- Kah LC, Riding R (2007) Mesoproterozoic carbon dioxide levels inferred from calcified cyanobacteria. *Geology* **35**, 799–802.
- Kah LC, Grotzinger JP (1992) Early Proterozoic (1.9 Ga) thrombolites of the Rocknest formation, Northwest Territories, Canada. *Palaos* **7**, 305–315.
- Kaplan A, Reinholt L (1999) The CO₂-concentrating mechanism of photosynthetic microorganisms. *Annual Review of Plant Physiology and Plant Molecular Biology* **50**, 539–570.
- Kappler A, Newman DK (2004) Formation of Fe(III)-minerals by Fe(II)-oxidizing photoautotrophic bacteria. *Geochimica et Cosmochimica Acta* **68**, 1217–1226.
- Kappler A, Pasquero C, Konhauser KO, Newman DK (2005) Deposition of banded iron formations by anoxygenic phototrophic Fe(II)-oxidizing bacteria. *Geology* **33**, 865–868.
- Karl DM, McMurtry GM, Malahoff A, Garcia MO (1988) Loihi Seamount, Hawaii: a mid-plate volcano with a distinctive hydrothermal system. *Nature* **335**, 532–535.
- Kasting JF (1987) Theoretical constraints on oxygen and carbon dioxide concentrations in the Precambrian atmosphere. *Precambrian Research* **34**, 205–229.

- Kelts K, Hsü KJ (1978) Freshwater carbonate sedimentation. In: *Lakes Chemistry, Geology, Physics* (ed. Lerman A). Springer, New York, pp. 295–323.
- Kempe S, Kazmierczak J (1994) The role of alkalinity in the evolution of ocean chemistry, organization of living systems, and biocalcification processes. *Bulletin de la Institut Océanographique (Monaco)* **13**, 61–117.
- Kendall B, Reinhard CT, Lyons TW, Kaufman AJ, Poulton SW, Anbar AD (2010) Pervasive oxygenation along late Archean ocean margins. *Nature Geoscience* **3**, 647–652.
- Kenward PA, Goldstein RH, González LA, Roberts JA (2009) Precipitation of low-temperature dolomite from an anaerobic microbial consortium: the role of methanogenic Archaea. *Geobiology* **7**, 556–565.
- Kiessling W (2002) Secular variations in the Phanerozoic reef ecosystem. In: *Phanerozoic Reef Patterns* (eds Kiessling, W, Flügel E, Golonka J). SEPM Special Publication, No. 72, Tulsa, OK, pp. 625–690.
- Klein C, Beukes NJ, Schopf JW (1987) Filamentous microfossils in the early Proterozoic Transvaal Supergroup: their morphology, significance, and paleoenvironmental setting. *Precambrian Research* **36**, 81–94.
- Knoll AH, Semikhatov MA (1998) The genesis and time distribution of two distinctive Proterozoic stromatolite microstructures. *Palaios* **13**, 408–422.
- Konhauser KO (1998) Diversity of bacterial iron mineralization. *Earth-Science Reviews* **43**, 91–121.
- Konhauser KO (2000) Hydrothermal bacterial biomineratation: potential modern-day analogues for Precambrian banded iron formation. In: *Marine Authigenesis: From Global to Microbial* (eds Glenn CR, Lucas J, Prévôt L). SEPM Special Publication No. 66, Tulsa, OK, pp. 133–145.
- Konhauser KO (2007) *Introduction to Geomicrobiology*. Blackwell, Oxford, 425pp.
- Konhauser KO, Hamade T, Morris RC, et al. (2002) Did bacteria form Precambrian banded iron formations? *Geology* **30**, 1079–1082.
- Konhauser KO, Newman DK, Kappler A (2005) The potential significance of microbial Fe(III) reduction during deposition of Precambrian banded iron formations. *Geobiology* **3**, 167–177.
- Konhauser KO, Lalonde SV, Amskold L, Holland H (2007) Was there really an Archean phosphate crisis? *Science* **315**, 1234.
- Konhauser KO, Pecoits E, Lalonde SV, et al. (2009) Oceanic nickel depletion and a methanogen famine before the Great Oxidation Event. *Nature* **458**, 750–753.
- Krom MD, Berner RA (1980) Adsorption of phosphate in anoxic marine sediments. *Limnology and Oceanography* **25**, 797–806.
- Liang L, McNabb JA, Paulk JM, Gu B, McCarthy JF (1993) Kinetics of Fe(II) oxygenation at low partial pressure of oxygen in the presence of natural organic matter. *Environmental Science and Technology* **27**, 1864–1870.
- Logan BW (1961) Cryptozoan and associated stromatolites from the Recent, Shark Bay, Western Australia. *Journal of Geology* **69**, 517–533.
- Lovley DR (1990) Magnetite formation during microbial dissimilatory iron reduction. In: *Iron Biominerals* (eds Frankel RB, Blakemore RP). Plenum Press, New York, pp. 151–166.
- Lowenstam HA (1981) Minerals formed by organisms. *Science* **211**, 1126–1131.
- Lyons WMB, Long DT, Hines ME, Gaudette HE, Armstrong PB (1984) Calcification of cyanobacterial mats in Solar Lake, Sinai. *Geology* **12**, 623–626.
- Mandernack KW, Tebo BM (1993) Manganese scavenging and oxidation at hydrothermal vents and vent plumes. *Geochimica et Cosmochimica Acta* **57**, 3907–3923.
- Merz MUE (1992) The biology of carbonate precipitation by cyanobacteria. *Facies* **26**, 81–102.
- Merz-Preiß M, Riding R (1999) Cyanobacterial tufa calcification in two freshwater streams: ambient environment, chemical thresholds and biological processes. *Sedimentary Geology* **126**, 103–124.
- Michaelis W, Seifert R, Nauhaus K, et al. (2002) Microbial reefs in the Black Sea fuelled by anaerobic oxidation of methane. *Science* **297**, 1013–1015.
- Miller AG, Colman B (1980) Evidence for HCO_3^- transport in the blue-green alga (cyanobacterium) *Coccochloris peniocystis*. *Plant Physiology* **65**, 397–402.
- Monty CLV (1976) The origin and development of cryptalgal fabrics. In: *Stromatolites* (ed. Walter MR), *Developments in Sedimentology*, Vol. 20, Elsevier, Amsterdam, pp. 193–249.
- Moore LS, Burne RV (1994) The modern thrombolites of Lake Clifton, Western Australia. In: *Phanerozoic Stromatolites II* (eds. Bertrand-Sarfati J, Monty C). Kluwer, Dordrecht, pp. 3–29.
- Morris RC (1993) Genetic modelling for banded iron-formation of the Hamersley Group, Pilbara Craton, Western Australia. *Precambrian Research* **60**, 243–286.
- Morse JW, Casey WH (1988) Ostwald processes and mineral paragenesis in sediments. *American Journal of Science* **288**, 537–560.
- Myers KH, Nealson KH (1988) Bacterial manganese reduction and growth with manganese oxide as the sole electron donor. *Science* **240**, 1319–1321.
- Nielson AE, Söhnle O (1971) Interfacial tensions electrolyte crystal-aqueous solutions, from nucleation data. *Journal of Crystal Growth* **11**, 233–242.
- Pentecost A (1987) Growth and calcification of the freshwater cyanobacterium *Rivularia haematites*. *Proceedings of the Royal Society of London, Series B* **232**, 125–136.
- Pentecost A (2005) *Travertine*. Springer, Berlin, 445pp.
- Pigott JD, Land LS (1986) Interstitial water chemistry of Jamaican reef sediment: sulfate reduction and submarine cementation. *Marine Chemistry* **19**, 355–378.
- Planavsky NJ, Rouxel O, Bekker A, Lalonde SV, Konhauser KO, Reinhard CT, Lyons T (2010) The evolution of the marine phosphate reservoir. *Nature* **467**, 1088–1090.
- Plée K, Ariztegui D, Martini R, Davaud E (2008) Unravelling the microbial role in ooid formation – results of an in situ experiment in modern freshwater Lake Geneva in Switzerland. *Geobiology* **6**, 341–350.
- Posth NR, Hegler F, Konhauser KO, Kappler A (2008) Alternating Si and Fe deposition caused by temperature fluctuations in Precambrian oceans. *Nature Geoscience* **1**, 703–707.
- Pratt BR (1982) Stromatolite decline – a reconsideration. *Geology* **10**, 512–515.
- Price GD, Sültemeyer D, Klughammer B, Ludwig M, Badger MR (1998) The functioning of the CO_2 concentrating mechanism in several cyanobacterial strains: a review of general physiological characteristics, genes, proteins and recent advances. *Canadian Journal of Botany* **76**, 973–1002.

- Rashby SE, Sessions AL, Summons RE, Newman DK (2007) Biosynthesis of 2-methylbacteriohopanepolyols by an anoxic phototroph. *Proceedings of the National Academy of Sciences, USA* **104**, 15099–15104.
- Reid RP, Visscher PT, Decho AW, et al. (2000) *Nature* **406**, 989–992.
- Revbech NP, Jørgensen BB, Blackburn TH, Cohen Y (1983) Microelectrode studies of the photosynthesis and O₂, H₂S and pH profiles of a microbial mat. *Limnology and Oceanography* **28**, 1062–1074.
- Ridgwell AJ, Kennedy MJ, Caldeira K (2003) Carbonate deposition, climate stability, and Neoproterozoic ice ages. *Science* **302**, 859–862.
- Riding R (1977) Calcified Plectonema (blue-green algae), a recent example of Girvanella from Aldabra Atoll. *Palaeontology* **20**, 33–46.
- Riding R (1982) Cyanophyte calcification and changes in ocean chemistry. *Nature* **299**, 814–815.
- Riding R (1993) Interaction between accretionary process, relative relief, and external shape in stromatolites and related microbial deposits. *International Alpine Algae Symposium and Field-Meeting*, Munich–Vienna, August 29–September 5, 1993, Abstracts.
- Riding R (2000) Microbial carbonates: the geological record of calcified bacterial-algal mats and biofilms. *Sedimentology* **47**, 179–214.
- Riding R (2006) Microbial carbonate abundance compared with fluctuations in metazoan diversity over geological time. *Sedimentary Geology* **185**, 229–238.
- Riding R (2008) Abiogenic, microbial and hybrid authigenic carbonate crusts: components of Precambrian stromatolites. *Geologia Croatica* **61/2–3**, 73–103.
- Riding R (2009) An atmospheric stimulus for cyanobacterial-bioinduced calcification ca. 350 million years ago? *Palaios* **24**, 685–696.
- Riding R, Liang L (2005a) Geobiology of microbial carbonates: metazoan and seawater saturation state influences on secular trends during the Phanerozoic. *Palaeogeography, Palaeoclimatology, Palaeoecology* **219**, 101–115.
- Riding R, Liang L (2005b) Seawater chemistry control of marine limestone accumulation over the past 550 million years. *Revista Española de Micropaleontología* **37**, 1–11.
- Riding R, Awramik SM, Winsborough BM, Griffin KM, Dill RF (1991) Bahamian giant stromatolites: microbial composition of surface mats. *Geological Magazine* **128**, 227–234.
- Robbins LL, Blackwelder P (1992) Biochemical and ultrastructural evidence for the origin of whiting. A biologically induced calcium carbonate precipitation mechanism. *Geology* **20**, 464–468.
- Robbins EI, LaBerge GL, Schmidt RG (1987) A model for the biological precipitation of Precambrian iron formations-B: morphological evidence and modern analogs. In: *Precambrian Iron-Formations* (eds Appel PWU, LaBerge GL). Theophrastus, Athens, Greece, pp. 97–139.
- Robbins LL, Tao Y, Evans CA (1997) Temporal and spatial distribution of whiting on Great Bahama Bank and a new lime mud budget. *Geology* **25**, 947–950.
- Roberts JA, Bennett PC, González LA, Macpherson GL, Milliken KL (2004) Microbial precipitation of dolomite in methanogenic groundwater. *Geology* **32**, 277–280.
- Rost B, Riebesell U, Burkhardt S, Sültemeyer D (2003) Carbon acquisition of bloom-forming marine phytoplankton. *Limnology and Oceanography* **48**, 55–67.
- Sassen R, Roberts HH, Carney R, et al. (2004) Free hydrocarbon gas, gas hydrate, and authigenic minerals in chemosynthetic communities of the northern Gulf of Mexico continental slope: relation to microbial processes. *Chemical Geology* **205**, 195–217.
- Sheldon ND (2006) Precambrian paleosols and atmospheric CO₂ levels. *Precambrian Research* **147**, 148–155.
- Schultze-Lam S, Beveridge TJ (1994) Nucleation of celestite and strontianite on a cyanobacterial S-layer. *Applied and Environmental Microbiology* **60**, 447–453.
- Sherman AG, James NP, Narbonne GM (2000) Sedimentology of a late Mesoproterozoic muddy carbonate ramp, northern Baffin Island, Arctic Canada. In: *Carbonate Sedimentation and Diagenesis in the Evolving Precambrian World* (eds Grotzinger JP, James NP). SEPM Special Publication, No. 67, Tulsa, OK, pp. 275–294.
- Shinn EA, Steinen RP, Lidz BH, Swart PK (1989) Perspectives. Whiting, a sedimentologic dilemma. *Journal of Sedimentary Petrology* **59**, 147–161.
- Søgaard EG, Medenwaldt R, Abraham-Peskir JV (2000) Conditions and rates of biotic and abiotic iron precipitation in selected Danish freshwater plants and microscopic analysis of precipitate morphology. *Water Research* **34**, 2675–2682.
- Srdić D, Horvatinčić N, Obelić B, Kračar I, Slepčević A (1985) Calcite deposition processes in karst waters with special emphasis on the Plitvice Lakes Yugoslavia. *Carsus Jugoslaviae* **11**, 101–204.
- Steefel CI, Van Cappellen P (1990) A new kinetic approach to modeling water-rock interaction: the role of nucleation, precursors, and Ostwald ripening. *Geochimica et Cosmochimica Acta* **54**, 2657–2677.
- Straub KL, Benz M, Schink B, Widdel F (1996) Anaerobic, nitrate-dependent microbial oxidation of ferrous iron. *Applied Environmental Microbiology* **62**, 1458–1460.
- Straub KL, Benz M, Schink B (2001) Iron metabolism in anoxic environments at near neutral pH. *FEMS Microbial Ecology* **34**, 181–186.
- Stumm W, Morgan JJ (1996) *Aquatic Chemistry*, 3rd edn. John Wiley & Sons, Inc., New York.
- Summons RE, Jahnke LL, Hope JM, Logan GA (1999) 2-Methylhopanoids as biomarkers for cyanobacterial oxygenic photosynthesis. *Nature* **400**, 554–557.
- Sumner DY (1997) Late Archean calcite-microbe interactions: two morphologically distinct microbial communities that affected calcite nucleation differently. *Palaios* **12**, 302–318.
- Sumner DY, Grotzinger JP (2004) Implications for Neoarchean ocean chemistry from primary carbonate mineralogy of the Campbellrand-Malmani Platform, South Africa. *Sedimentology* **51**, 1273–1299.
- Swett K, Knoll AH (1985) Stromatolitic bioherms and microphytolites from the Late Proterozoic Draken Conglomerate Formation, Spitsbergen. *Precambrian Research* **28**, 327–347.
- Templeton AS, Knowles EJ, Eldridge DL, et al. (2009) A seafloor microbial biome hosted within incipient ferromanganese crusts. *Nature Geoscience* **2**, 872–876.
- Thompson JB (2000) Microbial whiting. In: *Microbial Sediments* (eds Riding R, Awramik SM). Springer-Verlag, Berlin, pp. 250–260.

- Thompson JB, Ferris FG (1990) Cyanobacterial precipitation of gypsum, calcite, and magnesite from natural alkaline lake water. *Geology* **18**, 995–998.
- Thompson JB, Ferris FG, Smith DA (1990) Geomicrobiology and sedimentology of the mixolimnion and chemocline in Fayetteville Green Lake, New York. *Palaios* **5**, 52–75.
- Trendall AF (2002) The significance of iron-formation in the Precambrian stratigraphic record. *Special Publication from the International Association of Sedimentology* **33**, 33–66.
- Trichet J, Défarge C (1995) Non-biologically supported organomineralization. *Bulletin de l'Institut Océanographique de Monaco* **14**, 203–236.
- van Gemerden H (1993) Microbial mats: a joint venture. *Marine Geology* **113**, 3–25.
- Van Lith Y, Warthmann R, Vasconcelos C, McKenzie JA (2003a) Sulfate-reducing bacteria induce low-temperature Ca-dolomite and high Mg-calcite formation. *Geobiology* **1**, 71–80.
- Van Lith Y, Warthmann R, Vasconcelos C, McKenzie JA (2003b) Microbial fossilization in carbonate sediments: a result of the bacterial surface involvement in dolomite precipitation. *Sedimentology* **50**, 237–245.
- van Veen WL, Mulder EG, Deinema MH (1978) The *Sphaerotilus-Leptothrix* group of bacteria. *Microbiology Reviews* **42**, 329–356.
- Visscher PT, Stoltz JF (2005) Microbial mats as bioreactors: populations, processes, and products. *Palaeogeography, Palaeoclimatology, Palaeoecology* **219**, 87–100.
- Walcott CD (1914) Cambrian geology and paleontology III: Precambrian Algonkian algal flora. *Smithsonian Miscellaneous Collection* **64**, 77–156.
- Walker JCG (1984) Suboxic diagenesis in banded iron formations. *Nature* **309**, 340–342.
- Walter MR, Veevers JJ, Calver CR, Gorjan P, Hill AC (2000) Dating the 840–544 Ma Neoproterozoic interval by isotopes of strontium, carbon, and sulfur in seawater, and some interpretative models. *Precambrian Research* **100**, 371–433.
- Warthmann R, Van Lith Y, Vasconcelos C, McKenzie JA, Karpoff A-M (2000) Bacterially induced dolomite precipitation in anoxic culture experiments. *Geology* **28**, 1091–1094.
- Weber KA, Churchill PF, Urrutia MM, Kukkadapu RK, Roden EE (2006b) Anaerobic redox cycling of iron by wetland sediment microorganisms. *Environmental Microbiology* **8**, 100–113.
- Williams RJP (1981) Physico-chemical aspects of inorganic element transfer through membranes. *Philosophical Transactions of the Royal Society of London* **B294**, 57–74.
- Xiong J (2006) Photosynthesis: what color was its origin? *Genome Biology* **7**, 2451–2455.
- Zahnle KJ, Claire MW, Catling DC (2006) The loss of mass-independent fractionation of sulfur due to a Paleoproterozoic collapse of atmospheric methane. *Geobiology* **4**, 271–283.